IMAGING CERVICAL SPECIMENS FOR PRE-CANCER SCREENING WITH MULTI-FREQUENCY ELECTRICAL IMPEDANCE TOMOGRAPHY TECHNIQUE

NAPATSAWAN NGAMDI

Graduate School Srinakharinwirot University

2022

การสร้างภาพชิ้นเนื้อปากมดลูกสำหรับการตรวจคัดกรองมะเร็งปากมดลูกด้วยเทคนิคการสร้างภาพความนำไฟฟ้าด้วยการวัดหลายความถี่

นภัสวรรณ์ งามดี

ปริญญานิพนธ์นี้เป็นส่วนหนึ่งของการศึกษาตามหลักสูตร
วิศวกรรมศาสตรมหาบัณฑิต สาขาวิชาวิศวกรรมชีวการแพทย์
คณะวิศวกรรมศาสตร์ มหาวิทยาลัยศรีนครินทรวิโรฒ
ปีการศึกษา 2565

IMAGING CERVICAL SPECIMENS FOR PRE-CANCER SCREENING WITH MULTI-FREQUENCY ELECTRICAL IMPEDANCE TOMOGRAPHY TECHNIQUE

NAPATSAWAN NGAMDI

A Thesis Submitted in Partial Fulfillment of the Requirements

for the Degree of MASTER OF ENGINEERING

(M.Eng. (Biomedical Engineering))

Faculty of Engineering, Srinakharinwirot University

2022

THE THESIS TITLED

IMAGING CERVICAL SPECIMENS FOR PRE-CANCER SCREENING WITH MULTI-FREQUENCY ELECTRICAL IMPEDANCE TOMOGRAPHY TECHNIQUE

BY

NAPATSAWAN NGAMDI

HAS BEEN APPROVED BY THE GRADUATE SCHOOL IN PARTIAL FULFILLMENT
OF THE REQUIREMENTS FOR THE MASTER OF ENGINEERING
IN M.ENG. (BIOMEDICAL ENGINEERING) AT SRINAKHARINWIROT UNIVERSITY

(Assoc. Prof. Dr. Chatchai Ekpanyaskul, MD.)
Dean of Graduate School

ORAL DEFENSE COMMITTEE

..... Major-advisor
(Assoc. Prof. Dr.Taweechai Ouypornkochagorn)

..... Chair
(Assoc. Prof.Boon-ek Yingyongnarongkul)

..... Committee
(Assoc. Prof.Theekapun Charoenpong)

Title	IMAGING CERVICAL SPECIMENS FOR PRE-CANCER SCREENING WITH MULTI-FREQUENCY ELECTRICAL IMPEDANCE TOMOGRAPHY TECHNIQUE
Author	NAPATSAWAN NGAMDI
Degree	MASTER OF ENGINEERING
Academic Year	2022
Thesis Advisor	Associate Professor Dr. Taweechai Ouypornkochagorn

Screening for precancerous cervical cells can reduce the risk of death. However, most screening methods require laboratory investigation involving equipment, time, and expertise of pathologists. Electrical Impedance Tomography (EIT) is a method that possibly be used to localize cervical intraepithelial neoplasia (CIN), as the conductivity of the abnormality is typically higher than normal tissue. This study investigated this possibility and investigated a configuration of Multi-frequency EIT (mfEIT) Two electrode probes were developed. The experimental results showed that the system SNRs were more than 88 dB. The frequency of 50kHz and that of 10kHz are recommended for mfEIT reconstruction. The conductivity of formalin was approximately 0.586 S/m at 50 kHz excitation. The conductivity of the cervical specimens was 0.377 S/m in cases of abnormal tissue and 0.283 S/m in normal tissue, at 50 kHz excitation. Furthermore, the conductivity of the soft tissue was approximately 0.406 S/m at 50 kHz excitation, close to abnormal tissue. Image reconstruction results on three specimens found that the abnormality can be located. In the images, the region where the conductivity changes over different frequency indicated the location of abnormality or the region of the transformation zone or the endocervical region. Further experiments also found that the reconstruction images obtained with the single frequency EIT method where the measurement at the stroma region was used as the reference. This is because the back of the cervical specimen has the similar electrical characteristic as the soft and abnormal Therefore, the probe can detect abnormality using both single and multiple frequency basis, as the large conductivity change represents the normal region and the small conductivity change represents the abnormal region.

Keyword : Electrode probe, Cervical precancerous tissues, Reconstruction, Tissue conductivity

ACKNOWLEDGEMENTS

I would like to express my deep and sincere gratitude to my thesis advisor, Assoc. Prof. Dr. Taweechai Ouypornkochagorn, for giving me the opportunity to conduct research and for providing invaluable guidance and assistance throughout this endeavor. His attitude, vision, sincerity, and motivation have deeply inspired me.

Studying for a master's degree was challenging for me. It required more responsibility and time management skills, as well as the need to learn and grow independently. Without all the support that I have received from my advisor, I would not have achieved this far, and this thesis would not have been completed. He taught me the methodology to carry out research and to present the research works as clearly as possible. It was a great privilege and honor to work and study under his guidance. I am extremely grateful for what he has offered me. I would also like to thank him for his teaching and advice, not only on research methodologies but also on many other life methodologies.

I would like to extend our gratitude to the physician, Therdkiat Trongwongsa, M.D., and technician, Miss Jaruwan Sriwilai, for providing valuable information in the pathology laboratory, as well as for their invaluable technical support and assistance. Without their help, this study would not have been possible.

I would also like to express my heartfelt appreciation to my family, who supported me throughout my academic journey. Their unwavering love, encouragement, and understanding have been instrumental in helping me overcome the challenges of pursuing a master's degree. Their unwavering support has touched me deeply, and I am grateful for their constant presence in my life.

NAPATSAWAN NGAMDI

TABLE OF CONTENTS

Page

LIST OF TABLES

Page

LIST OF FIGURES

Page

CHAPTER 1
INTRODUCTION

1.1 Background

Cervical cancer is one leading cause of death in women around the world. In 2020, cervical cancer is the fourth most common cancer in women with an estimated 604,000 new cases and 432,000 deaths. About 90% of cases occurred in low– and middle-income countries [(1)] due to public health factors and limited access to treatment. Precancerous cervical screening at least once a year can reduce the risk to death by early treatment before abnormal tissues progress to cancer. The precancerous cervical lesion is the cervical cell dividing abnormally from a small area that could eventually develop into cervical cancer. Precancerous cells are classified according to the stage of abnormality development in epithelial which is called Cervical Intraepithelial Neoplasia (CIN). The precancerous cervical screening methods are commonly used to help identify the stage of CIN. There are many methods for cervical screening e.g. Pap smear test, liquid-based cytology, pelvic examination, colposcopy[(2)]. A Pap smear test or Papanicolaou smear is the most popular method. This method uses a spatula to take a tissue sample from cervix and smear the spatula on the slide and then the slide is immersed in 95% ethanol. The slide is read for abnormality investigation. This method is cheap and simple but it has a low sensitivity of about 51%. Liquid-based cytology is an improvement of Pap smear method. This method collects the tissue sample in the same way as Pap smear method but the spatula is put into methanol-based solution and is sent to an automated machine (for centrifugation and sedimentation purpose) to prepare the sample to be free of contaminants and for cell suspension. The accuracy of this method higher that the Pap smear method i.e., 66% but the cost is higher. In the case of pelvic examination, the physician inserts two gloved fingers inside the vagina while pressing down on the abdomen for evaluating the uterus. This method requires experts to do. Screening by colposcopy uses colposcope to magnifying images of the cervix. This method has many benefits for both screening and further diagnosis.

After the initial screening in a pathological laboratory, if abnormality is found, physicians will make a treatment plan whether using drug or carrying chemotherapy. In some cases, a biopsy of the cervix and relevant tissues may be required to determine the stage of abnormality and/or to remove the abnormal tissue. There are several methods of biopsy. Cone biopsy is using a scalpel or laser to remove a large cone-shaped tissue from cervix. Loop Electrosurgical Excision Procedure (LEEP) is another method using an electric wire loop to cut cervical biopsies. Specimen will be investigated by pathologists through the process of clinical diagnosis. Specimen will be further cut into thin pieces and entered the process of making slide for microscope investigation. These processes require experience, time and they are relevant with many equipment. Usually, it requires at least 14 days before the patient ready to be informed the result.

Rather than using the pathological methods mentioned above, screening based on electrical impedance measurement is another potential method as well[3]. The electrical impedance of normal tissue is usually higher than abnormal tissue due to the change of the cell shape (larger) and the lining within the cells (loosing the cell density). This allows more current to flow through the lining-up abnormal cells than that of the normal cells. This results in a decrease in cell impedance of the abnormal tissue[3]. Screening with impedance measurement basis uses an electrode probe or an electrode-array plate to measure. Abdul S, Brown BH, Milnes P, Tidy JA (2006) [4]proposed a 4-electrode probe to determine the presence of CIN by measuring the impedance at eight locations in a specimen. The average of impedance values was used to determine CIN is 3.84 - 5.35 Ωm and 19 Ωm for the normal tissue [4, 5]. Recently, image of conductivity distribution has been used for CIN localization based on Electrical Impedance Tomography (EIT) technique [6, 7]. EIT is a technique to create an image by collecting information from the injection current throughout the boundary and difference of voltage measurement on the boundary[8]. The measurement of impedance. Impedance measurements at various locations at different current patterns were used to reconstruct the image of conductivity distribution. This technique helps to reduce the

need of experience pathologists, and also reduce time and the need of using many equipment. Ousub S, et al (2021)[7] showed a simulation investigation to use a 9-electrode probe for localizing 1-2 mm diameter of CIN1 and CIN2/3 with the accuracy 0.92 mm in average. Zhang T, et al (2021) [9] improved the probe to have 16 electrodes and operate at 0.625-100 kHz frequency range. The probe was verified with phantom experiment (on a carrot piece in saline) and it can be obtained the tissue impedance in several orientation of measurement. Sillaparaya A, Ouypornkochagorn T (2021)[6] proposed the use of electrode-array plate to create the image of whole specimen. Two electrode layouts were investigated in this study by simulation with two 16-electrode configurations. The circular layout was reported to achieve the better localization performance location compared to the star layout.

EIT has been used in several medical applications. For examples lung imagine, breast imaging, brain imaging, monitor heart activity, prostate cancer[10-13]etc. Imaging the conductivity distribution with simple single-frequency EIT has a crucial limitation to need the measurement information at reference state. More specifically in cervical screening, the measurement when there is no abnormality must be early performed as the reference state. This is practically difficult to obtain this information. Even though the missing of the early measurement might be replaced with the use of the measurement of different specimen or the use of the simulation data, this will cause error on reconstruction image. Multi-frequency Electrical Impedance Tomography technique (MFEIT) has been proposed to deal with this limitation. Two (or more) measurements at different frequencies will be performed. The voltage measurement at high frequency is used as the reference measurement instead. The definition of the EIT image will be changed from the image of conductivity change over two periods over time to be the image of conductivity difference between two frequencies. Usually, the conductivity is changed when the frequency change – conductivity increases when the frequency is increased. The difference of conductivity changes over frequencies of the normal and the abnormal tissue will be highlighted in the image. With this principle, the measurement before CIN or cancer appear will be not needed. Because MFEIT allows

to reconstruct images of the cervix before the presence of CIN. It is important to note that imaging cervical specimen with a probe based on MFEIT has not been proposed to date. In this study, a development of EIT probes for MFEIT reconstruction was carried out. In this study, two EIT probes for MFEIT reconstruction were developed. The first probe has 7 electrodes and the other has 16 electrodes, where the probe diameter is 15 mm and the electrode diameter is 0.9 mm. The pattern of current injection and voltage measurement were investigated as well as the suitable measurement position on specimens. Five frequencies of current excitation were applied between 2 kHz and 125 kHz. The amplitudes of current inject were also investigated. The probe was evaluated with a tank experiment and phantom experiments. Five cervical specimens were investigated with the 16-electrode probe in accordance with the pathological diagnosis.

1.2 Objectives

1.2.1 To study the configuration and the reconstruction technique of multi-frequency Electrical Impedance Tomography method for cervical precancerous screening.

1.2.2 Design and build a suitable electrode probe for detecting cervical precancerous region in a specimen.

1.3 Scope

1.3.1 Detect precancerous squamous cell carcinoma of the cervix based on MFEIT.

1.3.2 Study and design a mathematical model of cervical tissue in according to the LEEP method (Loop Electrosurgical Excision Procedure).

1.3.3 Use a 7-electrode probe and 16-electrode of 15 mm probe diameter and 0.9 mm electrode diameter.

1.3.4 Use Electrical Impedance Tomography and Diffuse Optical Tomography Reconstruction Software (EIDORS (http://eidors3d.sourceforge.net/)) for forwarding calculation.

1.3.5 Use the Clementine EIT machine to experiment with specimens with the frequency between 2-125kHz and the current below 2mArms.

CHAPTER 2

THEORY AND LITERATURE REVIEW

2.1 Cervical cancer

Cervical cancer is the abnormal cell that develops in the cervix, the lowest of the uterus. The cervix is the passage of menstrual blood. This area is often the beginning of cervical cancer before it spreads to other areas, such as the ovaries.

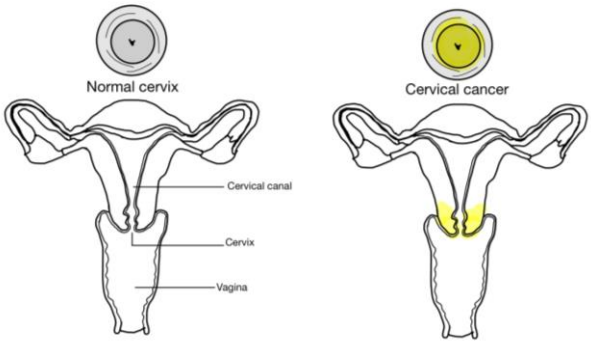

Figure 1 Cervical cancer

The abnormal cells usually occur in the transformation zone (TZ) [14] is the connection between the Ectocervix, which consists of the squamous cells, and the Endocervix, which consists of the glandular cells. The Transformation zone can be classified into 3 types depending on the location which is varied from person to person.

1. Type 1 TZ, is located on the ectocervix only. 360-degree visual inspection is possible as the entire ectocervix is visible inside the vagina.

2. Type 2 TZ, partly located in the ectocervix and partially in the endocervical canal, so colposcopy can still be performed.

3. Type 3 TZ is located in the endocervical canal or the internal os of the cervix. This type of transformation zone is difficult to observe with the eye. Conical biopsy (LEEP) is often needed to investigate. [14, 15]

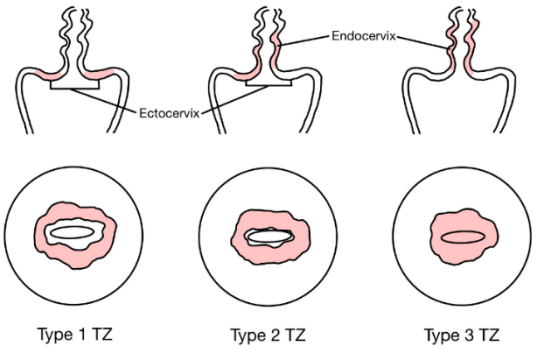

Figure 2 Type of transformation zone

2.1.1 Cervical Cancer Types

1. Squamous cell carcinoma is the most common type of cervical cancer. It starts as a thin and flat cell and occurs on the outer surface of the cervix.

2. Cervical mucosal cancer (adenocarcinoma) is rare, which is a cancer that is mutated from mucous gland cells. It is shaped like a pillar in the line of the cervical canal. [16]

2.1.2 Symptom

Cervical cancer in its early stages is asymptomatic. It will show symptoms when the cancer is in the advanced stage, such as vaginal bleeding, bleeding after or during sex or after menopause, pus-filled white discharge, vagina smelling abnormal, pelvic pain, or pain during sex. [16]

2.1.3 Etiology

Cervical cancer is caused mainly by infection with HPV (human papillomavirus) through sexual intercourse and other causes that are risk factors for cervical cancer, such as smoking, having multiple sexual partners, having many children, immunodeficiency, etc. If the body has been infected with HPV, it cannot be eliminated. Normal cells then transform into abnormal cells, known as precancerous of the cervix (precancerous cervical cells).

2.1.4 Pathophysiology

Cervical cells are squamous cells that are arranged in layers of overlapping cells. Determination of pathological stages precancerous can be divided into 2 forms according to the characteristics of cell changes:

Cytology - Considered from properties, physiology, and organelle structure in cells. Cytology anomalies can be diagnosed in a variety of ways, including Liquid-Based cytology and HPV testing. Cytology anomalies can be explained with the stage of Squamous Intraepithelial Lesions (SIL) that consist of 2 stages:

- Low-grade SIL refers to the initial changes in the shape, size, and number of cells. The stage lesion may disappear by themselves but some may evolve into High-grade SIL.

- High-grade SIL means the endometrium has changed. If the abnormal cells only occur in the cervix, it can be determined as moderate or severe dysplasia.

Histology - Consider the histology of normal tissue by looking at the changes in the cells lining the cervix using a microscope. In principle, it divides the precancerous staging of Cervical Interepithelial Neoplasia (CIN) into 3 stages:

- CIN 1: cellular changes in approximately 1/3 of the cervical epithelium layer. If detected at this stage, up to 80% of patients can recover.

- CIN 2: Approximately 2/3 of the cellular changes from the lower layer lining the cervix.

- CIN 3: There are cellular changes along the thickness of the cervical mucosa. If left untreated, it will develop into cancer.[17]

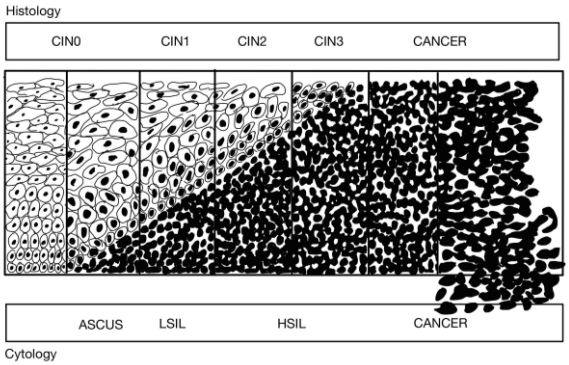

Figure 3 Stages of precancerous cervical cell.

2.1.5 Methods for screening cervical cancer

Pap smear

This is the first method used to screen for cervical cancer by using a vaginal speculum to insert through and spread the vagina. A tissue sample is then taken using a spatula and then smear on a slide and immersed in a cell treatment solution or immersed in 95% ethanol. Next, the slide is read for examining abnormalities and see if cervical cancer cells appear. This method is a simple and effective way to diagnose. [2]

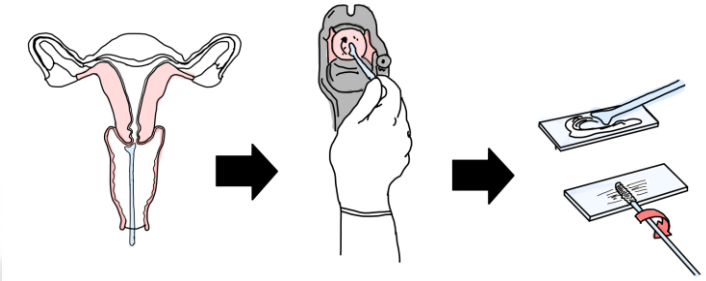

Figure 4 Pap smear

Liquid-based cytology

The process to take a sample is similar to the Pap smear method. The sample of cervical mucosa is taken out with a spatula. The spatula is shortened (by breaking at the joint) and is put in a bottle of tissue treatment solution before entering an automatic machine for preparing the tissues to be free from contamination and to reduce the density of cells when smear on the slide. This process may be repeated if necessary.[18]

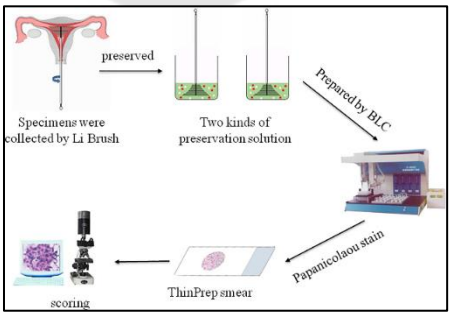

Figure 5 Liquid-based cytology

Source:https://journals.plos.org/plosone/article/figure?id=10.1371/journal.pone.0190851.g001

Pelvic examination

Pelvic examination is an important method of detecting cervical cancer. The physician inserts two gloved fingers inside the vagina. While simultaneously pressing down on the abdomen for evaluating the uterus, ovaries, and other pelvic organs through the fingers.

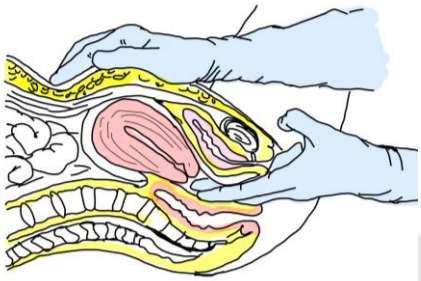

Figure 6 Pelvic examination

Colposcopy

This is an examination of the cervix by magnifying images of the ectocervix, squamocolumnar junction (SCJ), and the endocervical canal using an instrument called a colposcope. The doctor will insert a speculum to stretch the vagina and a topical solution is applied to the cervix to whiten the abnormal cells. The doctor can then view the cells using a microscope to check for abnormal cells. This method is not only used for preliminary screening, but also for determining the need to do further diagnosis. This method is necessary for diagnostic curettage or cone biopsy, endocervical curettage, LLETZ/LEEP operation.[2]

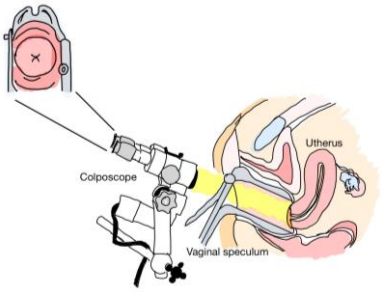

Figure 7 Colposcopy

2.1.6 Management and treatment

Cervical cancer usually develops slowly and also CIN may take many years before developing to cancer. The abnormal cells that occur may disappear on their own or become cancerous cells. Most cervical cancer is caused by Human Papilloma Virus (HPV) infection, of which there are more than 100 types and about 12 types lead to cancer. [19] Typically, a preliminary screening is performed at the first step such as a Pap smear or liquid-based cytology. If the screening test results show abnormality, the process of treatment will be assessed according to the stage of the lesion. Initially, abnormal tissues are removed from the cervix, and the surround tissues may also be taken out if cancer is suspected that it may spread. There are many methods for cervical biopsy in which cold knife cone biopsy and Loop electrosurgical excision procedure (LEEP) are the most preferred methods. The taken or removal tissue will be next examined in a pathological laboratory If the laboratory confirms it is cancerous, further tests will be performed to determine the spread of cancer. Treatment planning will depend on the stage, age, and general health condition of patients. The treatments could be radiation, chemotherapy, surgery, targeted therapy, and immunotherapy. The methods for cutting out abnormal or suspicious tissues are as follows:

Cold knife cone biopsy

Cone biopsy uses a scalpel or laser to remove a large cone-shaped tissue from the cervix.[20] This type of biopsy allows to get to the deeper layers of cervix[21]. It can detect cervical dysplasia that could to cancer.

LEEP (Loop electrosurgical excision procedure)

LEEP is the use of an electric wire loop to cut cervical biopsies. General, the physician will cut cervical biopsies with the approximate diameter of 15-20 mm while the thickness is 3-5 mm.

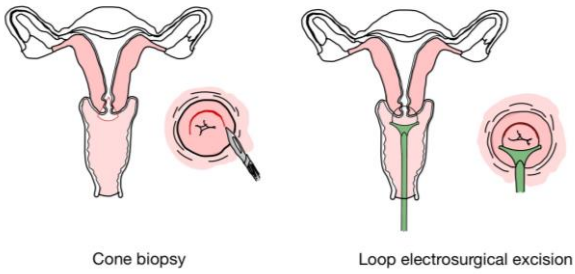

Figure 8 Cold knife (left) and LEEP (right) method.

Hysterectomy

Hysterectomy is one of the treatments for Cervical Dysplasia, which is a pre-cancer stage of the cervix, or wide and deep abnormalities that hard to be cured by removing the uterus and relevant tissues. [22] Although this therapy can make patients effectively recovering from the illness, but doctors often use this method as a last resort since the patient will not be able to have children again. This may cause vaginal discharge or blood and decreasing in hormone levels as well.

2.2 Pathological examination

Pathological examination is the process or method for examining organs, tissues, cells, or secretions from the human including those from the bodies of the deceases. The examination is based on the naked eye examination and microscopic inspection in combination with other techniques such as immunohistochemistry and biomolecules. The examination can be divided into 3 categories: surgical pathological examination, cytological examination, and autopsy. The examination that involves with bulk tissue and relates with this study is surgical pathological examination. The surgical pathological diagnosis involves the naked eye examination by looking at a microscope. This includes other special examinations by which the specimen can be a small piece of specimens obtained from a puncture laparoscopic surgery or the whole organ. The example of the examination procedure is shown in Figure 9.

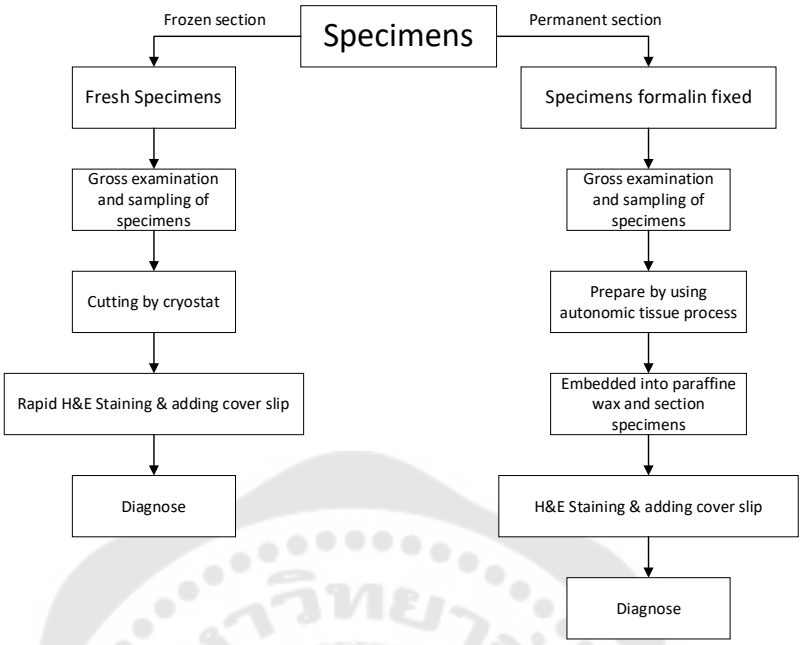

Figure 9 Work flow of surgical pathological examination.

The specimens to be examined must be soaked in tissue-healing solution to maintain the tissue condition allow to be stored for a long time and for the ease of tissue hardening that is necessary in the process of tissue sliding. It also help in dying process. The popular tissue-healing solution is 10% phosphate-buffered formalin. It is clear and colorless liquid but has pungent smell. This solution is suitable for soaking all types of tissues.

In addition, the orientation of the specimens must be specified to ensure mutual understanding between the referring physician and the pathologist. To determine the orientation of specimens, suture is used as the marker on the specimens. At least 2 markers with different number of knots, number of ties, or different length of residue suture end are usually put with 90 degrees apart. For example, the first marker is located at the superior margin with long residue suture end and the second marker is at the lateral margin with short residue suture end.

Biopsy examination

Biopsy examination is start with gross examination which is based on bare eyes inspection to obtain diagnostic information such as appearance, size,

weight, and color. The markers could be put on the biopsy specimens to indicate the specimen orientation. The specimens are next put into a paraffin block and then put in an automatic tissue processing machine for at least 12 hours. After finish the paraffin process, the specimens are ready for slide diagnosis by microscope that carry out by pathologists. [23]

For example, of a cervical LEEP specimen examination, the orientation is indicated by needles or suture as shown in Figure 10 – the markers were put at 12 o'clock and 6 o'clock. The specimen is then divided into four pieces, according to the clock face, at 12-3 o'clock, 3-6 o'clock, 6-9 o'clock and 9-12 o'clock. Each piece is put into a cartridge and proceeds with the method explained above. In some cases, specimens may not be circular in shape, be separated (Figure 11) or be dented., This will cause difficulties and require more time to process.

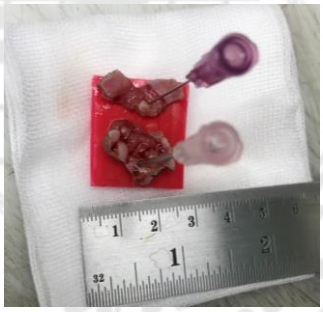

Figure 10 Specifying the orientation of the specimen by using needles.

Figure 11 The set of specimens to investigate.

2.3 Bioelectrical impedance

2.3.1 Bioelectrical impedance of biological tissue

The tissue consists of a group of structured cells having similar functions. Tissues can be classified into four groups, according to the composition of the cell: epithelial tissues, endothelial tissues, stroma tissues, and connective tissues. Epithelial tissues are the cells that envelop the body and membranes of internal organs. Endothelial tissues are cells that are inside the internal organs. Stroma tissues consist of cells that act as a matrix for other cells to be embedded. Connective tissues act as a link from one tissue to another. Cells and tissues of living things like the human body are organized into a three-dimensional array with a complex structure. Biological tissue consists of intracellular fluids (ICF) that is covered with cell membranes and extracellular fluids (ECF) where the cells are suspended. Tissue impedance is frequency-dependent to an alternating electrical source that is different due to the ability of the electric current can pass through each kind of fluid and the cell membrane [18]. At a certain frequency, the impedance is different on different tissue depending on the cell structure, cell lining, and water composite, and then the impedance can be used to determine the abnormality of cells and cell structure. There are many medical applications those are based on electrical impedance measurement such as bioelectrical impedance analysis (BIA), electrical impedance spectroscopy (EIS), electrical impedance plethysmography (IPG), impedance cardiography (ICG), and electrical impedance tomography (EIT).

2.3.2 Screening cervical precancerous tissues with electrical impedance measurement

Abdul S, Brown BH, Milnes P, Tidy JA (2006) [4, 24] proposed a 4-electrode probe to detect precancerous cervical based on electrical impedance measurement. The electrodes in the probe were 5.5 mm in diameter. The excitation current was 20 μA magnitude in 2-1200 kHz of frequency. The impedance of the normal tissue was found different to that of the precancerous tissue. However, this method cannot distinguish CIN 1 from mature metaplasia cells in the frequency range of approximately 100 Hz - 10 kHz.

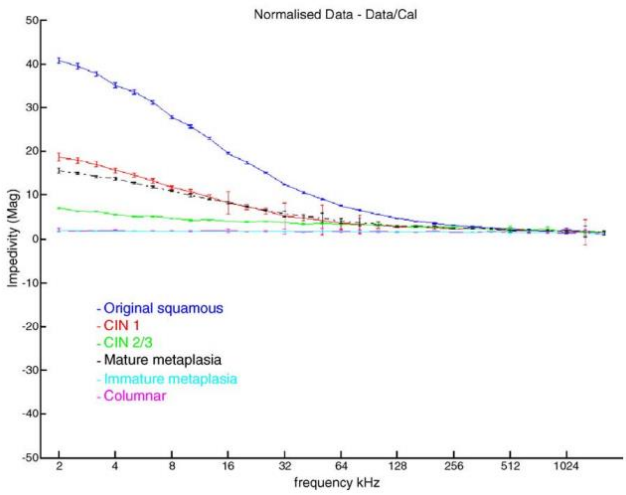

Figure 12 Impedance spectra measured on different types of cervical biopsies [4].

According to Figure 12, the impedance of abnormal tissue is smaller than that of normal tissue (blue line) at low frequency that lower than 10kHz, and less different in higher frequency.

In addition, Das L, Das S, and Chatterjee J (2015) [3]proposed to use a planar electrode plate which is eight well arrays with one electrode per well (Figure 13) for studying the electrical characteristics of cervical tissue. The measurement on several regions can be collected simultaneously. Cervical samples were taken by smearing then bioimpedance was measured using the planar-electrode plate with a frequency of 100 Hz to 1 MHz and 10 mV of AC voltage. The impedance of the normal samples was found that higher than that of the abnormal samples. The impedance decreased when the frequency was increased (Figure 14). In the case of abnormal samples, the impedance was smaller than that of the normal samples and it was slightly changed when the frequency was over 10kHz. [3]

Figure 13 Specialized 8-well ECIS device.[3]

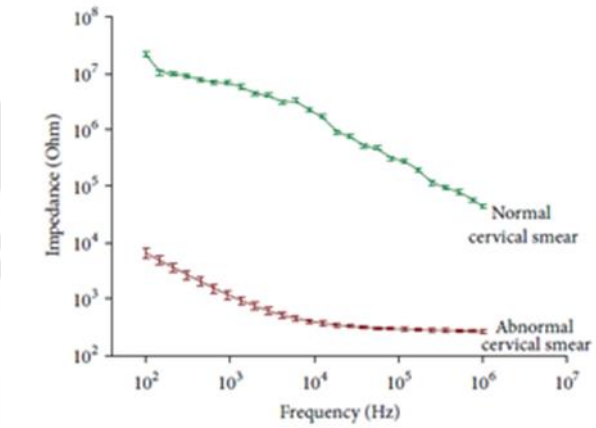

Figure 14 Differences in the impedance of normal and abnormal tissue in the frequency range of 100 – 1MHz[3]

2.3.3 Electrical impedance tomography (EIT)

As mentioned in previous section, biological impedance can be used to identify abnormal tissues because the space between cells is larger than the normal cells, the size of the nucleus is larger and the internal structure of the cells is rearranged to be loosen. When the abnormal tissue has fewer layers of cell lining resulting in the allowance of current running through the cells easier i.e. the impedance reduces in value. Conductivity is used to determine the stage of abnormal tissue which is inversely proportional to the electrical impedance. The current (I) is injected to measure the corresponding voltage (V) in regard to the equation V=IR where I is a constant if the current source is implemented and V is a constant when the voltage source is applied.

Electrical impedance tomography (EIT) is a biomedical imaging technology that is non-invasive and can reconstruct images from the electrical impedances obtained from different locations. In the image reconstruction, forward problem and inverse problem are used together to create the image of conductivity distribution that can be used to locate abnormal tissue. Forward problem has conductivity (σ) as the main parameter to compute boundary voltage (V) where e is the measurement error and U is the model function (2.1). The conductivity is a function of frequency in regard to the Cole-Cole equation. Inverse problem or image reconstruction problem attempts to determine the location of the abnormal cell by using the boundary voltage information obtained from the experiment to estimate the conductivity distribution from the least different between the measurement voltage (V_{el}) and the computational voltage obtained from the model function ($U_{(\sigma)}$) as shown in equation (2.2).

$$V = U(\sigma) + e \tag{2.1}$$

$$\sigma = \arg\min_{\sigma} \left\{ || V_{el} - U_{(\sigma)} ||^2 \right\} \tag{2.2}$$

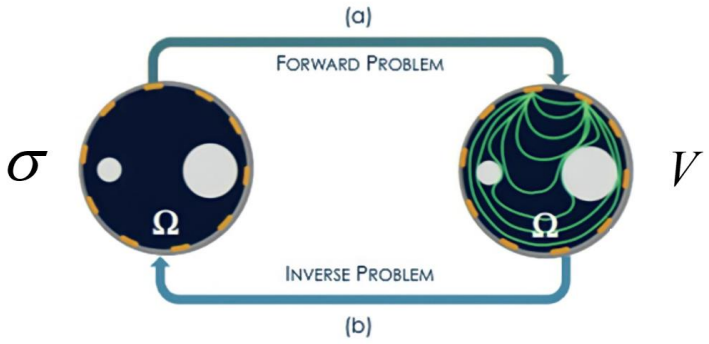

Figure 15 The relation between Forward problem (a) and Inverse problem (b).

Ousub S, et a (2021)[7]designed an electrode probe for screening CIN using Electrical Impedance Tomography technique. The electrode probe had 9 electrodes and 9 mm diameter of probe head. The electrodes had 1 mm in diameter. The current of 10 μA at the frequency of 100 Hz, 1 kHz, and 10 kHz was injected at a time. The result

shows that the probe can effectively locate the position of CIN. A limitation of the localization was reported in this study - the abnormal cells beneath the electrodes cannot be located.

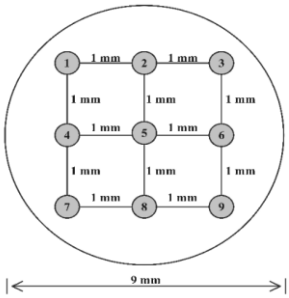

Figure 16 9-electrode layout proposed by Ousub S, et a (2021)[7]

Sillaparaya A and Ouypornkochagorn T(2021)[6] proposed to use a planer electrode array plate, consisting of 16 electrodes, for detecting cervical cancer of a 25mm-diameter specimen by using electrical impedance tomography technique. Based on simulation, two electrode layouts were investigated where the circular layout showed the better localization performance – lesser artifacts and capable to locate CIN situated at the edge of the specimen.

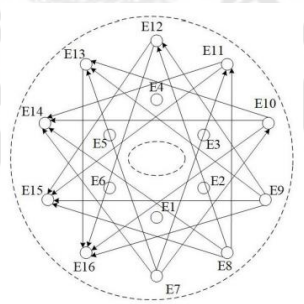

Figure 17positioning electrode of Circle layout and current pattern [6]

In addition, Zhang T, et al [9] developed a 17-electrode probe (one is used as ground) for detecting of cervical intraepithelial neoplasia (CIN). The diameter of the outer ring and the inner ring of electrode arrays was 10 mm and 6.67 mm respectively. The diameter of the electrode was 1 mm. The probe was designed to use with an

Electrical Impedance Spectroscopic (EIS) system where the current magnitude of between 85 μA and 310μA, and a fixed frequency of 0.625, 1, 5, 10, 50, and 100 kHz. However, this work has not shown the impedance or the image of cervical specimens, but the result on a phantom experiment was reported.

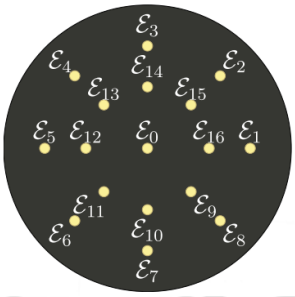

Figure 18 Electrode probe proposed by Zhang T, et al. [9]

2.3.4. Multifrequency Electrical impedance tomography (MFEIT)

Multifrequency electrical impedance tomography uses tissue impedance that differently changes over frequency to create an image of conductivity. An electrical current, at least 2 frequencies, is released into tissue and corresponding boundary voltage measurements are collected. MFEIT is based on frequency-difference principle where a measurement frequency is used as the reference to compare with the other measurement frequency. This is different to the traditional (or single frequency) EIT which is based on time-difference principle where the prior measurement must be performed. MFEIT is then allow for the imaging of an event without knowledge of a prior condition, This feature is necessary for the diagnosis of diseases such as acute stroke, brain injury, and breast cancer because most patients are admitted after the onset of pathological diseases. [25]

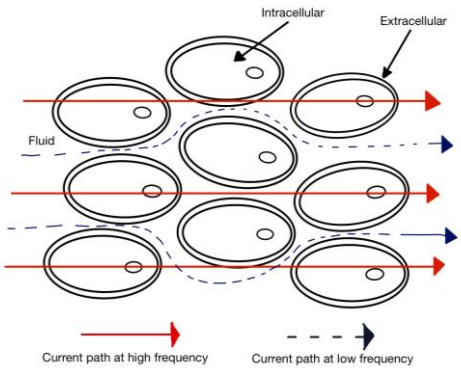

Figure 19 The current flow behavior over tissues at high-frequency and low-frequency.

Principle of Multi-frequency Electrical Impedance Tomography

Generally, time-difference (TD) electrical impedance tomography (EIT) is mathematical relation between the change of boundary voltage (ΔV) of a certain frequency (single frequency) and the change of conductivity distribution ($\Delta\sigma$) over time as in (2.3) where J is the Jacobian or sensitivity matrix.

$$\Delta V \approx J\Delta\sigma \tag{2.3}$$

The voltage value obtained from the first measurement (the prior state) is t_0 used as a reference value. The voltage value obtained from subsequent measurements is t_1 then taken into account with the reference value for reconstructing the different image, that can be calculated by (2.4)

$$\Delta V = V_{t_1} - V_{t_0} \tag{2.4}$$

In multi-frequency scenario or frequency-difference (FD) electrical impedance tomography, ΔV is now a pair of complementary currents with two different frequencies i.e., f_1 and f_2 (2.5). f_1 in this time is used as the reference frequency.

The voltage information obtained from both frequencies is considered together to reconstruct the image of the conductivity difference between 2 frequencies. The image of conductivity change in the FDEIT case can be estimated with (2.6) Where $H(\cdot)$ is the regularization function and λ is the regularization factor.

$$\Delta V = V_{f_1} - V_{f_2} \tag{2.5}$$

$$\Delta\hat{\sigma} = \arg\min_{\Delta\sigma}\left\{\frac{1}{2}\left\|\Delta V - J\Delta\sigma\right\|_2^2 + \lambda H\left(\Delta\sigma\right)\right\} \tag{2.6}$$

Multi-frequency electrical impedance tomography has been used in medicine For example, Goren N, et al (2018)[26],using MFEIT to collect data on stroke patients for establishing a classifier of predicting strokes.

2.3.5 Conductivity

Conductivity is the ability to conduct electric current. It can be obtained as the inverse of the electrical resistivity and the unit is S/m (siemens per meter). To compute the conductivity, it can be determined with the four-electrode method. Four electrodes are aligned in line, two end electrodes are used for current excitation, and the other two electrodes (in the middle) are used for voltage measurement. In the case of liquid, it can be calculated from (2.7). This method required a chamber with equal electrode distance. The contact area to the liquid must know as well.

$$\sigma = \frac{1}{R} = \frac{I}{V}\cdot\frac{A}{d} \tag{2.7}$$

Where R is resistivity

I is electric current.

V is the voltage.

A is the electrode area.

d is the distance between the electrode.

Four-point-probe theory for estimating conductivity on surface measurement

F.M. Smits [27] and D. Schroder[28], proposed that the four-point probe resistivity measurement is a useful tool for measuring the conductivity of semiconductors. The electrodes are put on the surface of measured material. This technique involves discharging current at the outer-end electrode pair and measuring voltage at the inner electrode pair to obtain surface conductivity measurements by calculating in (2.8) where $\frac{\pi}{\ln(2)} = 4.532$ and t is thickness of object.

$$\sigma = \frac{\pi}{\ln(2)} \frac{V}{I} t \tag{2.8}$$

The equation (2.8) works for thickness less than half the probe spacing. For thicker samples the formula becomes (2.9) from. [28]

$$\sigma = \frac{V}{I} \cdot \pi t \cdot \left(\ln \left(sinh\left(\frac{t}{s} \right) \cdot \left(sinh\left(\frac{t}{2s} \right) \right)^{-1} \right) \right)^{-1} \tag{2.9}$$

The four-point probe method with the equation above is used to measure conductivity with the assumption the area of the electrode's tips is very small. However, in this study, the contact area of electrodes was large compared to the electrode distance. As a result, in this work, a method was developed to measure conductivity by adding a factor ($F(t)$) into equation (2.9) as in (2.10), resulting in a conductivity value close to the actual value. Simulation result shows that if the thickness of sample was more than 5 mm, $F(t)$ is about to 1.

$$\sigma = F(t) \cdot \frac{V}{I} \cdot \pi t \cdot \left(\ln \left(sinh\left(\frac{t}{s} \right) \cdot \left(sinh\left(\frac{t}{2s} \right) \right)^{-1} \right) \right)^{-1} \tag{2.10}$$

Conductivity of cervical precancerous tissues

Electrical impedance of tissues can be based on the Cole-Cole plot. For EIT applications, resistance of tissue over frequency is of interest. Based on the equivalent electrical circuit of tissue as shown in Figure 20. Brown BH, et al (2000)[24] has reported the values of series resistance (R), shunt resistance (S), and series capacitance (C) of normal and abnormal cervical tissues as shown in Figure 21, These values can be used to create Cole-Cole plot as the formula (2.11) -(2.13). The estimate of impedance at a certain frequency then can be calculated by (2.14).

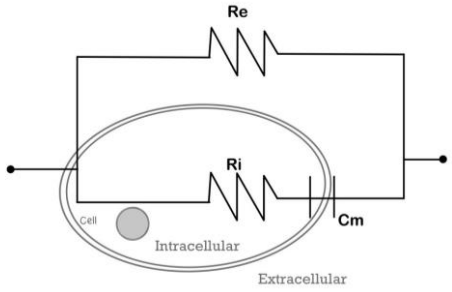

Figure 20 The equivalent electrical circuit

	Normal squamous epithelium (n=370)			CIN 1 (n=63)			CIN 2/3 (n=126)		
	R (Ω m)	S (Ω m)	C (μF/m)	R (Ω m)	S (Ω m)	C (μF/m)	R (Ω m)	S (Ω m)	C (μF/m)
Median and range									
Minimum	1·45	0·03	0·06	0·69	0·08	0·12	0·89	0·77	0·05
25th percentile	12·8	1·15	0·37	2·69	2·49	0·33	2·36	4·39	0·36
Median	20·1	1·91	0·65	3·27	4·53	0·66	2·98	6·08	0·64
75th percentile	26·8	2·78	1·20	5·52	6·31	1·46	4·22	7·63	1·09
Maximum	28·8	73·8	27·4	28·8	12·5	6·02	21·7	13·0	19·3
Mean									
Mean	19·0	2·31	1·12	5·36	4·79	1·01	3·85	6·10	1·01
SD	7·77	4·04	1·96	5·84	3·09	1·01	2·89	2·57	1·93
SE	0·40	0·21	0·10	0·73	0·38	0·12	0·25	0·22	0·17
95% CI									
Lower	18·2	1·90	0·92	3·88	4·02	0·76	3·34	5·64	0·67
Upper	19·8	2·72	1·32	6·83	5·57	1·27	4·36	6·55	1·35

Figure 21 The values of normal tissue and precancerous tissue of the cervical. [24]

$$R_0 = R \tag{2.11}$$

$$R_\infty = \frac{RS}{R+S} \tag{2.12}$$

$$F_c = \frac{1}{2\pi C\left(R+S\right)} \tag{2.13}$$

Where R_0 is resistance at zero frequency

R_∞ is resistance at the infinity frequency

F_c is frequency

R is impedance of the extracellular space

S is impedance of the intracellular space

C is capacitance of the cell membrane (μF/m).

$$Z = R_\infty + \frac{\left(R_0 - R_\infty\right)}{\left(1 + \left[jF / F_c\right]\right)^{1-\alpha}} \tag{2.14}$$

Where Z is Impedance at frequency F

F is the interested frequency

α is adjustment factor, usually is zero

2.3.6 Current injection and voltage measurement pattern

Current injection and voltage measurement pattern is relevant with the sensitivity to detect the conductivity change. For the single source EIT, the common used patterns are adjacent, cross, opposite [29], and trigonometric pattern.

Adjacent pattern

The current injection or the voltage measurement pattern using adjacent pattern is performed on adjacent electrode pairs. As shown in Figure 22, the example of adjacent injection is from pairs 1-2 and this causes the corresponding adjacent measurement pairs at the remaining electrodes, e.g., pair. 3-4 and 4-5 pairs. This method has highly sensitivity if there is a change of conductivity near the boundary region. By the way, the low sensitivity region is at in the middle region. [30]

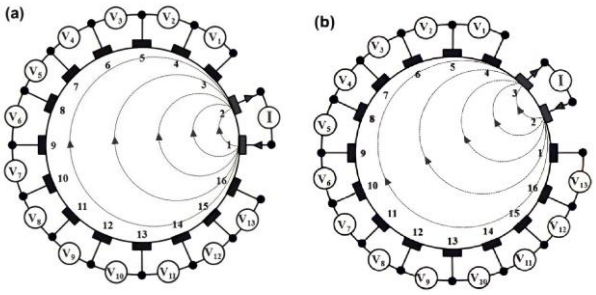

Figure 22 Adjacent current and measurement pattern

Cross pattern

This pattern performs a current injection or voltage measurement across or diagonally the electrodes. As the example in Figure 23, the current is injected from the electrode pair 16-2, and 13 pairs of voltage are measured using the 1st electrode as the reference position. This method will be highly sensitive in the middle area, better sensitive than the adjacent pattern but less sensitive than the adjacent for the boundary region. (30)

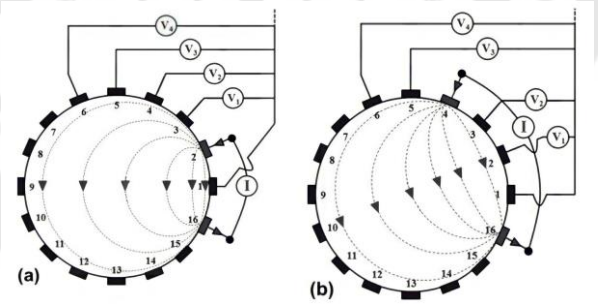

Figure 23 Cross pattern

Opposite pattern

This pattern performs a current injection or voltage measurement between opposite pairs of electrodes. As shown in Figure 24, the current is injected from pairs 1-9 and voltage is measured from the remaining electrodes respectively, e.g., 2-3 pairs, 2-4 pairs, and pairs. 2-5, etc. This pattern has improve sensitivity at the middle region compared to the other patterns. (30)

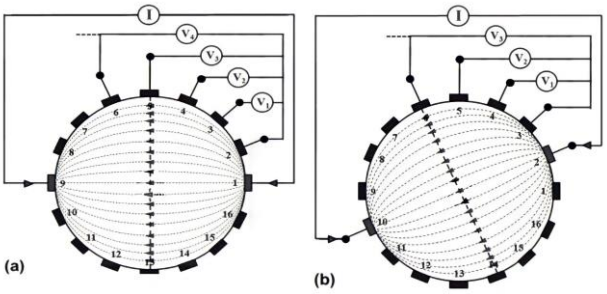

Figure 24 Opposite pattern

Trigonometric method

This pattern could be determined as an adaptive pattern where the angular injection and measurement is performed with a certain degree. For example, as shown in Figure 25, the current injection and voltage measurement pattern are similar in pattern but on the different pair. This pattern has been reported higher sensitivity than the previous patterns when the degree of electrode pair is approximately 90 degree. [31]

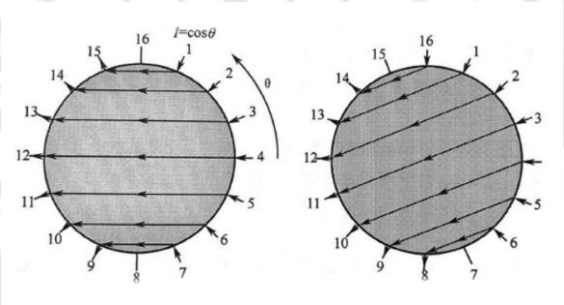

Figure 25 Trigonometric method [31]

2.3.7 Truncated Singular Value Decomposition (SVD) Reconstruction Technique

Singular Value Decomposition (SVD) has been used for image reconstruction. The reconstruction is based on (2.15) in according to (2.3) where the conductivity change ($\Delta\sigma$) is computed from the inverse of Jacobian matrix (J) and the boundary voltage change (ΔV). However, the Jacobian matrix is usually noninvertible since its size is the number of elements (n) and the number of measurements (m). The pseudo inversion is used. Regularization is also applied and the Tikhonov regularization is the simple method (2.16) where I is identity matrix and λ is the regularization parameter.

$$\Delta\sigma = J^{-1}\Delta V \tag{2.15}$$

$$\Delta\sigma = \left(J^T J + \lambda I\right)^{-1} J^T \Delta V \tag{2.16}$$

However, inverting the Jacobian term is computational expensive due to its size. Singular Value Decomposition (SVD) is used for reducing the computational resources. SVD decomposes the Jacobian matrix with (2.17) where U is an $m \times m$ unitary matrix, V is another $n \times n$ unitary matrix, and s is a $m \times n$ diagonal singular matrix keeping eigenvalues.

$$J = UsV^T \tag{2.17}$$

Using the traditional SVD causes a large matrix i.e., V where the matrix size is the square of the number of elements. Truncated SVD can reduce the size of the V matrix from $n \times n$ to $m \times n$. This is according that the size of s matrix can be reduced to $m \times m$ since there are only m eigenvalues in the s matrix (the eigenvalues only present at the diagonal of the matrix). Since the number of measurement (m) is substantially lower in number than the number of elements (in this research, the number of measurements is 240 and the number of elements is 26,930), using the truncated SVD then can reduce the need of computational resources. Furthermore, when substituting (2.17) to (2.16), it became (2.18) - (2.21). In (2.21), the term $\left(s^2 + \lambda I\right)$ is a diagonal matrix, then it can be easily to inverse.

$$\Delta\sigma = \left(\left(UsV^T\right)^T \left(UsV^T\right) + \lambda I\right)^{-1} \left(UsV^T\right)^T \Delta V \tag{2.18}$$

$$\Delta\sigma = \left(\left(Vs^T U^T\right)\left(UsV^T\right) + \lambda I\right)^{-1} \left(Vs^T U^T\right)\Delta V \tag{2.19}$$

$$\Delta\sigma = \left(s^T s + \lambda I\right)^{-1} \left(Vs^T U^T\right)\Delta V \tag{2.20}$$

$$\Delta\sigma = \left(s^2 + \lambda I\right)^{-1}\left(Vs^T U^T\right)\Delta V \tag{2.21}$$

2.3.8 Signal to Noise Ratio

Signal to Noise Ratio (SNR) is measure used in science and engineering which compares the level of the desired signal and the level of background noise and its unit of expression is typically decibels (dB). A high value of SNR indicates the higher level of signal compared to noise level. The equation to compute SNR is expressed in (2.18).

$$SNR = 20\log\left(\frac{V_s}{V_n}\right) \tag{2.18}$$

CHAPTER 3

RESEARCH METHODOLOGY

3.1 Simulation study

3.1.1 Mathematical model for reconstruction

A cervical finite element model was created based on the area of the electrode array that was placed onto the surface of the cervical specimen, created in a square shape. The model thickness was according to the thickness cervical specimen in Loop electrosurgical excision procedure (LEEP), 10 mm in width side and long side. The depth was set to 5 mm as a default value. However, the depth was changed depending on the thickness of the specimens. The model was created by NGSolve software. The top surface of the model represented cervical epithelium as shown in Figure 26, an example of model reconstruction with 5 mm of thickness. The number of elements was 26,930.

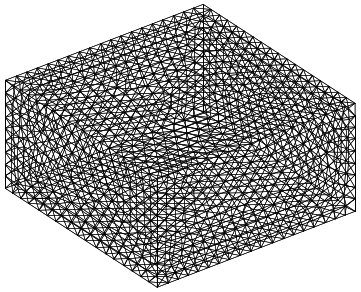

Figure 26 The model for reconstruction.

3.1.2 Electrode probe layouts and measurement positions on the created model

Two electrode probes were developed in this study with a probe diameter of 15 mm.Each probe has a different number of electrodes: the first one has 8 electrodes and the other one has 16 electrodes. All have a diameter of 0.9 mm. In the case of the 8-electrode probe, 7 of the electrodes are for image reconstruction, and 1 (an extra electrode) of them is used with the other electrode for measurement of the tissue conductivity only (according to the 4-point electrode method). Since the aim of the probes is for image reconstruction, we named the probe having 8 electrodes as “the 7-

electrode probe" (ignored the presence of the extra-electrode) and named the probe having 16 electrodes as "the 16-electrode probe". The diameter of the electrode array (in a circular shape) was 3.6 mm and 6.8 mm for the 7-electrode and the 16-electrode probe respectively (from the center of electrodes) (Figure 32, the extra-electrode does not appear in the model). The area of the electrode array is the sensitive region to detect the abnormality. Since LEEP biopsies typically have a diameter of 20 mm, the electrode array's area is suitable for imaging approximately 5.06% (7-electrode probe) to 14.82% (16-electrode probe) of the specimen region at a time. Therefore, the model reconstruction specifically focused on the area of the electrode array. The probe was designed to measure at the ectocervix cervix surface.

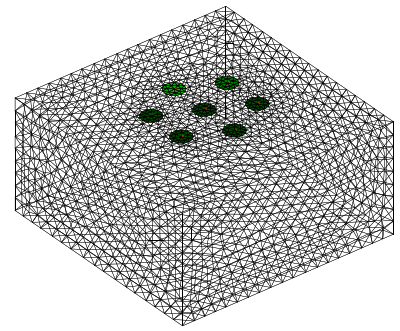

(a)

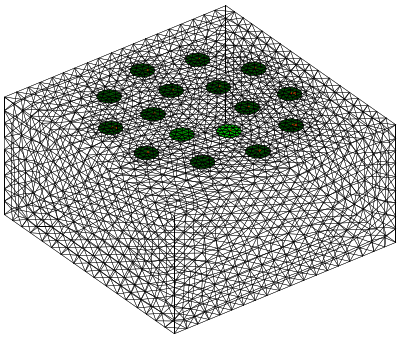

(b)

Figure 27 The model with (a) the 7-electrode probe and (b) the16-electrode probe measurement location.

3.1.3 Current injection and voltage measurement pattern

A current injection and voltage, measurement pattern was designed to meet with the electrode layout as shown in Figure 28 and Figure 29. The opposite current pattern was selected in the 7-electrode probe and the trigonometric current pattern was selected in the 16-electrode probe. The measurement pattern, adjacent was selected. The high sensitivity area is in the middle of the electrode layout because dense current pathways are there. The total of the current patterns was 20 for all probes. The number of composite measurements was 108 and 240 for the 7-electrode probe and the 16-electrode probe, respectively.

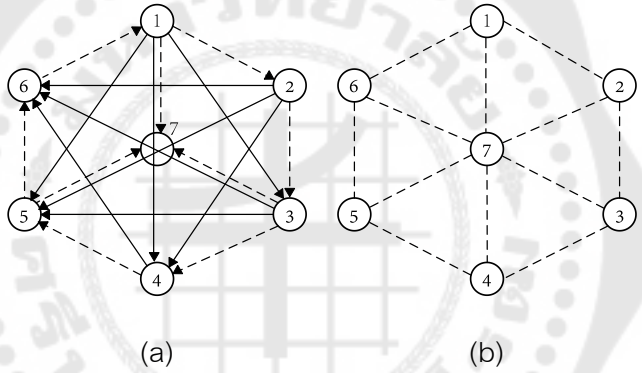

Figure 28 Current pattern (a) and measurement pattern (b) of the 7-electrode probe

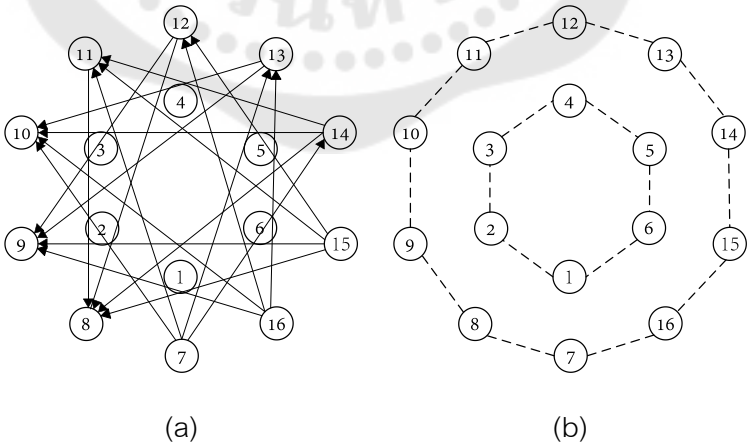

Figure 29 Current pattern (a) and measurement pattern (b) of the 16-electrode probe

3.1.4 Forward computation and reconstruction method

The current amplitude was determined by the settings of the EIT machine and was simulated at frequencies of 2 kHz, 10 kHz, 25 kHz, 50 kHz, and 125 kHz to compare the range of voltages with those obtained from the EIT machine. The forward computation was carried out by EIDORS software (http://eidors3d.sourceforge.net/). All the voltage information is used for reconstruction with the Singular Value Decomposition method (SVD). The regularization parameter was $1x10^{-4}$.

3.2 Experiment

3.2.1 Multiple-frequency EIT machine

The multiple-frequency EIT machine used in this study is “Clementine EIT” (Figure 31). The machine is capable to measure 32 channels with at least 80 dB SNR. The machine supports to inject fixed 5 frequencies of excitation current at 2, 10, 25, 50, 125 kHz at a time with selectable 2 sets of current amplitude i.e. 0.2, 1, 2, 2, 2 mArms respectively and 0.05, 0.2, 0.4, 0.4, 0.4 mArms respectively. The measurement gain is manually changeable with 1, 2, 3, and 10. The recording speed is 20 frames per second. The gain was set to 2 in this study.

3.2.2 Electrode probe

In this study, the author designed a new probe for use with the Clementine EIT, which is suitable for cervix application (Figure 31). The probe is circular in shape and has 7 and 16 electrodes with a diameter of 0.9 mm. The layout of the electrodes is based on the simulation described in Section 3.1.2. The 16-electrode probe, which has a 6.8 mm-diameter electrode array, was developed after the 7-electrode probe in order to cover a larger area on the surface of the cervical specimen. The diameter of the electrode array of the 7-electrode probe was 3.6 mm.

Figure 30 The clementine EIT machine.

(a) (b)

Figure 31 The electrode layout of the 7-electrode probe and the 16-electrode probe.

3.2.3 Phantom experiment

To verify the performance of the EIT machine, four experiments were performed. A 235-ohm resistor was used as a testing load (see Figure 32), at a channel of the machine, for investigating the machine and determining the SNR. A resistor phantom, as shown in Figure 34, was used to verify the gain and accuracy of the measurement (see Figure 35). Tank experiment was used for verifying the machine in the part of image reconstruction.

Figure 32 A 235-Ohm resistor connected to the machine.

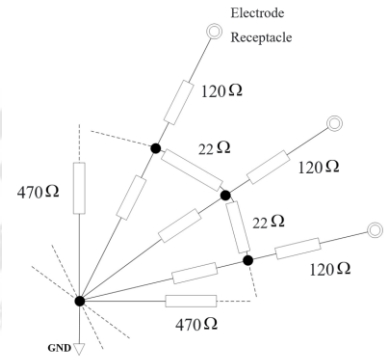

Figure 33 The circuit of the resistor phantom.

Figure 34 The resistor phantom connected to the machine.

In the tank experiment, a tank of 225-mm diameter with a height of 147 mm with 32 electrodes sticking around was used (but used only 16 electrodes). The saline was filled at the height of 120 mm where the conductivity of the saline was 0.249 S/m. Leads were connected from the machine to the tank (see Figure 38). A 38-mm diameter plastic rod was dipped in the tank. The voltage information was collected by Clementine EIT machine and the reconstruction method proposed in Section 3.1.4 was applied.

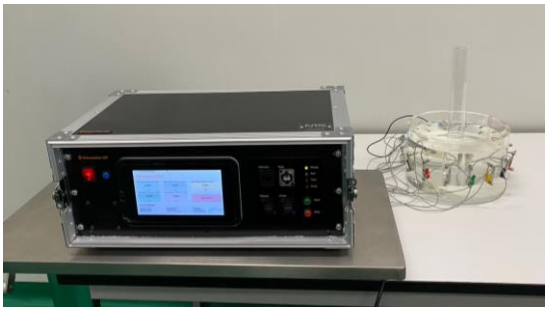

Figure 35 The tank connected to the machine.

In the 7-electrode probe validation, the probe was tested with a biomaterial sample. A chicken sausage was selected in this study by cutting in a circular shape of 19 mm diameter with 5 mm thickness. The sausage was kept in a sealed bag in a refrigerator and left outside with the bag at 25C room temperature for 30 minutes before the experiment onset. The EIT measurement was performed by attaching the electrode to the surface of the sausage, at the center, and recorded for 30 seconds. The probe was held in position with a grip holder attached to rods and a stand. The sausage was created a test marker by burning the sausage surface with a soldering iron. The tip size was 1.5 mm in diameter. The iron tip was first cleaned with new brass wool and isopropyl alcohol. The soldering iron was set at 380C and then the tip was gently pressed to the surface for 5 seconds. The surface was cleaned with a brush damped with 0.9% saline, and the measurement was performed again with the same procedure. The burning surface was expected to be seen in the reconstruction image. The burning surface was situated in different positions of the probe layout. There was only one burning marker on the sausage surface. The probe was moved into 3 positions as shown in Figure 36 and measured on the same piece of the burned sausage.

In the 16-electrode probe validation, the probe was tested with a biomaterial sample. A chicken sausage was selected in this study by cutting in a circular shape of 20 mm diameter with 5 mm thickness and putting a circular shape of cucumber on the surface of the chicken sausage. The testing sausage was placed in a plastic tray and did repeat twice. A chicken sausage was used immediately after taking it out from the package. The cucumber slice with a thickness of approximately 1-1.5 mm and a

diameter of 2 mm, 5 mm, or 10 mm was placed in 3 positions regarding the electrode layout (see Figure 38). Image reconstruction was be performed and the performance was evaluated by visualization.

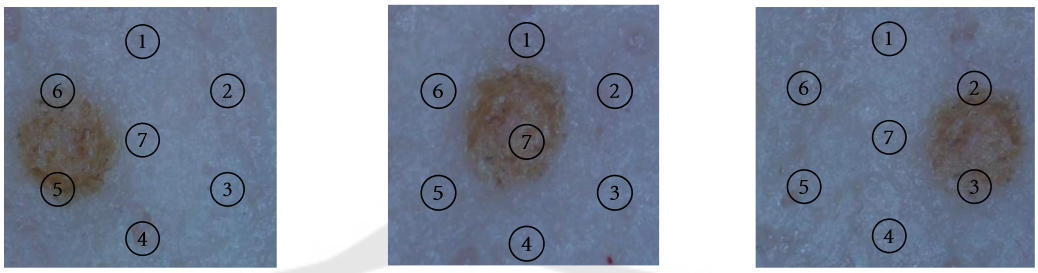

(a) Left (b) Center (c) Right

Figure 36 The position of burn marker.

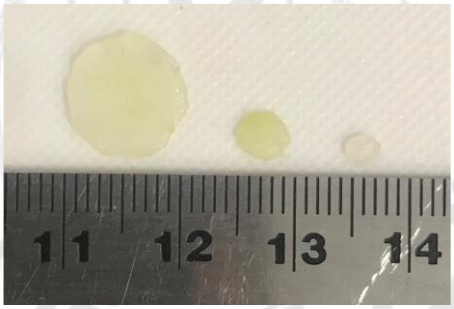

Figure 37 The 3 sizes of cucumber slices.

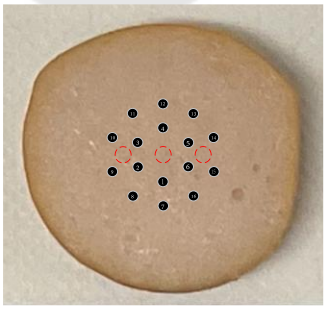

Figure 38 The position to place the cucumber slice on the surface of the chicken sausage.

3.2.4 Conductivity of the testing materials and the formalin solution

The background conductivity value is necessary for image reconstruction. All conductivity values used in this study were measured using the Clementine EIT machine and the measuring probes developed by the authors. The main target materials to evaluating the conductivity are the formalin solution (used in fixing the specimens), saline (used in the tank experiment), the tissue specimen, and the sausage.

The conductivity of formalin and that of the saline were measured with a chamber of 28x28x28 mm in size, developed by the author. The liquid was filled with the height from the bottom of the chamber of 8 mm. Four copper electrodes with a width of 15 mm dipping in the full depth were arranged with 3 mm separation (see Figure 39). The gap beside the electrode bar was filled with non-conductive foam sheets. The information for computing the conductivity has already been explained in Section 2.3.5.

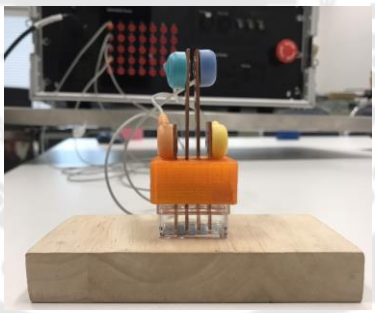

Figure 39 The chamber connected with The Clementine EIT.

The conductivity of chicken sausage and that of the specimens calculated based on the 4-electrodes method. The electrodes are aligned in a line with equal distance of separation. Two electrodes located at the both ends are used for current excitation and the other 2 electrodes are for voltage measurement. In the 7-electrode probe, the author added an extra-electrode for making an electrode line (see Figure 40(a)). The distance between each electrode is 1.8 mm (from the center to the center). For the 16-electrode, there is no perfect line where the electrodes are in line with equal

distance. The alignment that is closed as a line is displayed in Figure 40(b), which was used to measure conductivity in the specimen cases. The distance between electrodes in this imperfect alignment is 1.8 mm (that is the distance between the middle pair of the electrodes). The equation for estimating the conductivity has mentioned in Section 2.3.5.

Figure 40 The selection electrode used for estimating the conductivity.

3.2.5 Cervix experiment

Five cervix specimens fixed with formalin was investigated. The experiment took place at the Pathology department of the HRH Princess Maha Chakri Sirindhorn Medical Center and this experiment has been ethical approved by Human Research Ethics Committee of Srinakharinwirot University (SWUEC-097/2563). The experiment was done before the pathologist made a specimen diagnosis (Section 2.2). Physiological shape of cervical specimens was recorded first (e.g. diameter, thickness, marker, smear). The designed probe was measured in 4 quadrants (Figure 41-42) following the specimen manipulation process to make slides. The orifice was the reference of the quadrants. However, the measurement location (on epithelium) with the probes could be changed depending on the size of specimens. In each quadrant, 4 pieces of slices were made. The specimen was proceeded with pathological process until the result come out from pathologists to address the abnormality and the location of the abnormality. The measuring data was used in reconstruction and the reconstruction

images were used in comparison with the pathologist's diagnosis. The performance evaluation was based on visual inspection.

Since the probe should not be moved during the measurement and pressure on the measurement must be consistent when measuring cervical specimens, a stand was used to hold the probe steady and to apply pressure to the specimens (see Figure 42). The measurement duration was 60 seconds for each measurement. In some specimens, the back side of the epithelium was performed the measurement as well. The measurement data was used for verifying with the reconstruction based on the single frequency.

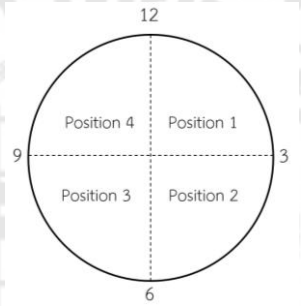

Figure 41 The quadrants assignment in a specimen.

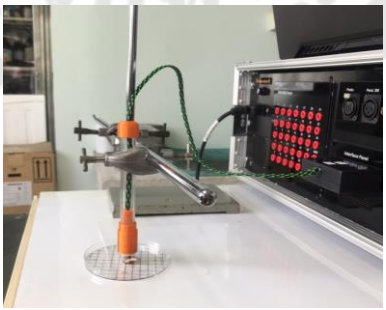

Figure 42 The example of measurement on cervical specimens with Clementine EIT.

CHAPTER 4
RESULT

4.1 Verification of the EIT machine

4.1.1 Signal to noise ratio test

This experiment tested how large of the machine noise compared to the signal. A 235 Ω resistor was used (Figure 36). The SNRs from this experiment were calculated using equation 2.18, of the gain x2 was used in this study.

Table 1 Signal to noise ratio.

Frequency(kHz)	SNR (dB)
2	77.13
10	88.88
25	90.63
50	88.94
125	86.44

Table 1 show the Clementine EIT machine can achieve the SNR more than 77 dB at frequency 2 kHz and more than 86 dB at frequency 10k, 25k, 50k, and 125k Hz.

4.1.2 Tank experiment

A tank of 225 mm-diameter with the height of 147 mm with 32 electrodes was used (only 16 electrodes were used in this study). The saline was filled with the height of 130 mm where the conductivity of saline was 0.249 S/m. A plastic rod with a diameter of 38 mm was dipped into the tank. The machine was set to 0.2, 1, 2, 2, and 2 mArms of current amplitude, with a measurement gain of 2 and a record duration of 60 seconds. The voltage comparison results are shown in Figure 43. The prediction voltage obtained from the model and the saline conductivity was simulated and compared to the measurement at different frequencies. The current amplitude set in the model was 2 mArms.

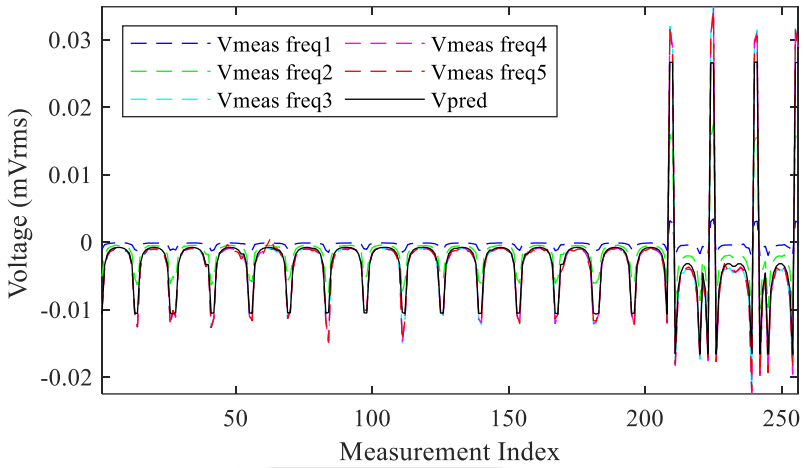

Figure 43 The Voltage measurement obtained from the tank experiment.

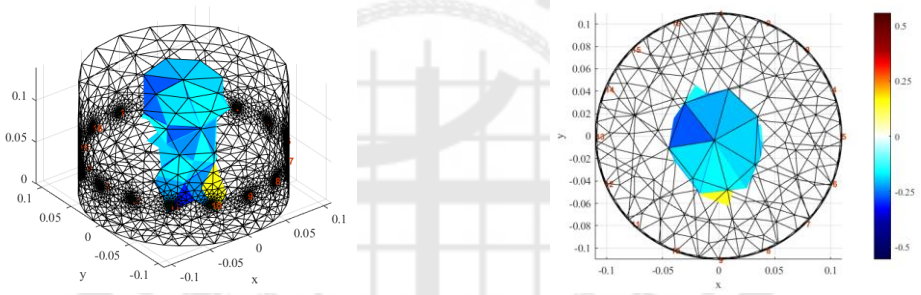

Side view Top view

Figure 44 Reconstruction image of the testing non-conductive rod, locating at the center of the tank. The reconstruction is based on the single frequency method.

In Figure 43, the comparison between the simulated voltage (Vpred) and the voltage (Vmeas) measured by the Clementine EIT is illustrated. It is obvious that all the measurements are consistent to the prediction. Figure 44 shows the reconstruction image of a tank with a plastic rod dipped in the center of the tank.

4.2 Conductivity

4.2.1 Conductivity of formalin

The conductivity of formalin was investigated in this study because it is relevant with the process of fixing cervix specimens. The 10% phosphate-buffered formalin is

use in this study. A chamber with four-electrode used in the measurement with the Clementine EIT machine. (Section 3.2.4)

Table 2 Voltage and conductivity of formalin.

Frequency(kHz)	Voltage (Vrms)	Conductivity(S/m)
2	0.013	0.127
10	0.019	0.346
25	0.027	0.492
50	0.023	0.586
125	0.021	0.639

4.2.2 The conductivity of cervical specimen

The previous study [4, 24] used in vivo measurements to determine the conductivity of cervical specimens, while this study used ex vivo specimens fixed in formalin for about 4 hours. The conductivity estimation is based on what is described in Section 2.3.5.(2.10).

Table 3 The conductivity of cervical specimen with 4 mm of thickness.

Frequency (kHz)	Conductivity (S/m) of normal cervical tissue (in vivo) Found in [4, 24]	Conductivity (S/m) of CIN2 tissue (in vivo) Found in [4, 24]	Conductivity(S/m) found in this study (ex vivo)							
			Case 3				Case 4		Case 5	
			Q1[3]	Q2[3]	Q3[1]	Q4[3]	Q1-4[4]	Q2-3[1]	Q1-4[2]	Q2-3[1]
2	0.0531	0.2607	0.251	0.295	0.157	0.364	0.228	0.170	0.269	0.184
10	0.0638	0.2811	0.273	0.324	0.177	0.381	0.244	0.197	0.306	0.203
25	0.1140	0.3390	0.302	0.354	0.217	0.409	0.263	0.235	0.341	0.227
50	0.2248	0.3891	0.353	0.398	0.282	0.459	0.299	0.299	0.406	0.269
125	0.4011	0.4170	0.545	0.522	0.472	0.639	0.447	0.563	0.608	0.391

[1] is the position of probe at squamous cell.

[2] is the position of probe at the soft tissue near orifice.

[3] is the position of probe at cancer.

[4] is the position of probe at CIN.

Table 4 The Conductivity(S/m) at the back of cervical specimen.

Frequency(kHz)	Conductivity(S/m) found in this study (ex vivo)	
	Case4	Case5
2	0.223	0.337
10	0.236	0.359
25	0.253	0.386
50	0.284	0.434
125	0.422	0.584

The conductivity of the cervix specimen found in this study is considerately larger than the in vivo measurement, in particular at the low frequency. This may due to

the influence of formalin immerse. Additionally, the pressure put on the specimens during the measurement could lead to the difference in conductivity as well.

Based on Table 3, in Case 3 quadrant 4 (Q4), which corresponds to the abnormality area (as shown in Figure 45), has a higher conductivity compared to the other quadrants. This is because the position of voltage measurement is located on the abnormality area. Similarly, in Case 5, even though there is no abnormality, quadrants 1-4 (Q1-4) have higher conductivity values because the position of voltage measurement is on the soft tissue near the orifice.

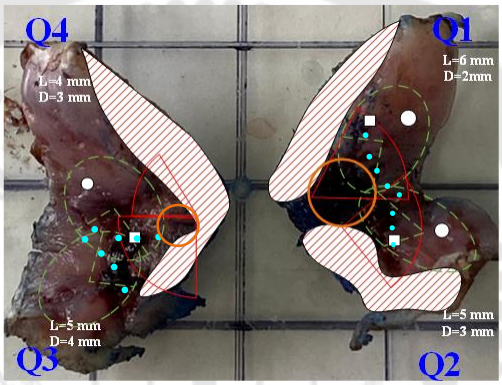

Case 3

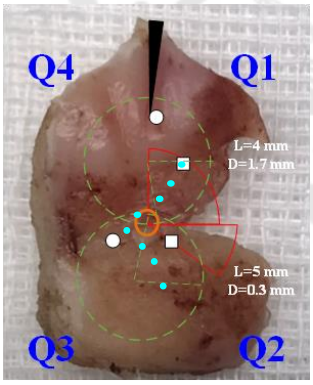

Case 4

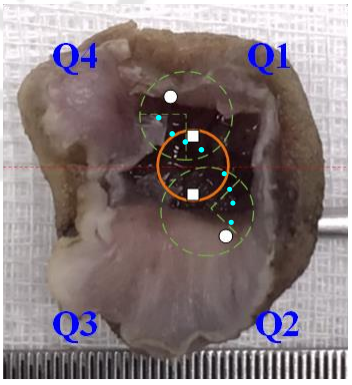

Case 5

Figure 45 The position of voltage measurement (blue point). The area within the red line indicates the area of abnormality, and the green line shows the location of the probe tip. The orange circle is the region of the soft tissue at the orifice.

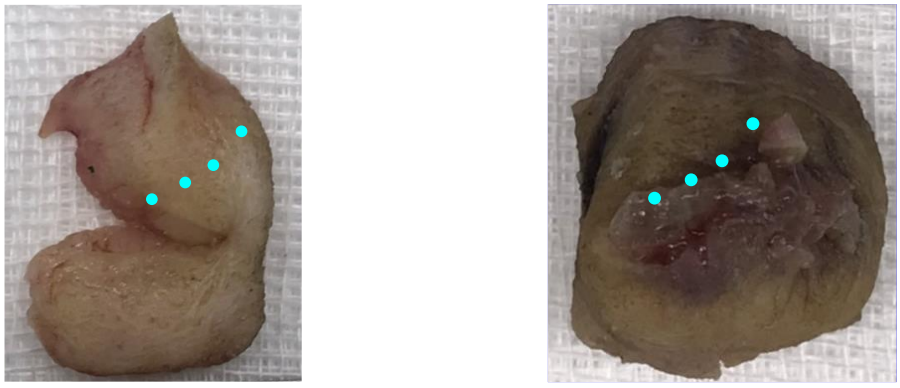

(a) (b)

Figure 46 The position of voltage measurement at the back of cervical specimen, (a) Case 4, (b) Case 5.

4.3 Phantom test

The phantom experiment test with a chicken sausage. Cutting in a circular shape of 25 mm diameter with 5 mm thickness. The investigation was performed on the 7-electrode probe and the 16-electrode probe. In the case of 7-electrode probe, the sausage was burned with an iron tip for few seconds in 3 locations : left, center, right. In the case of 16-electrode probe, and put a cucumber slice was put on the surface of sausage by cutting in a circular shape of 3 size as 2-mm, 5-mm, and 10-mm diameter with 1-1.5 mm thickness. Using for the 16-electrode probe and the burn marker was made for the 7-electrode probe. The voltage measurement is according to the current injection pattern and voltage measurement pattern in section 3.1.3 as shown in Figure 47-48, and can reconstructed image of the burn marker and the cucumber on sausage surface as in Figure 49-50. Please noted that the 16-electrode probe case was used based on for the multi-frequency measurements, with a frequency pair of 50 kHz and 10 kHz. On the other hand, the 7-electrode probe case was based on used for the single-frequency measurements, with 5 different frequencies.

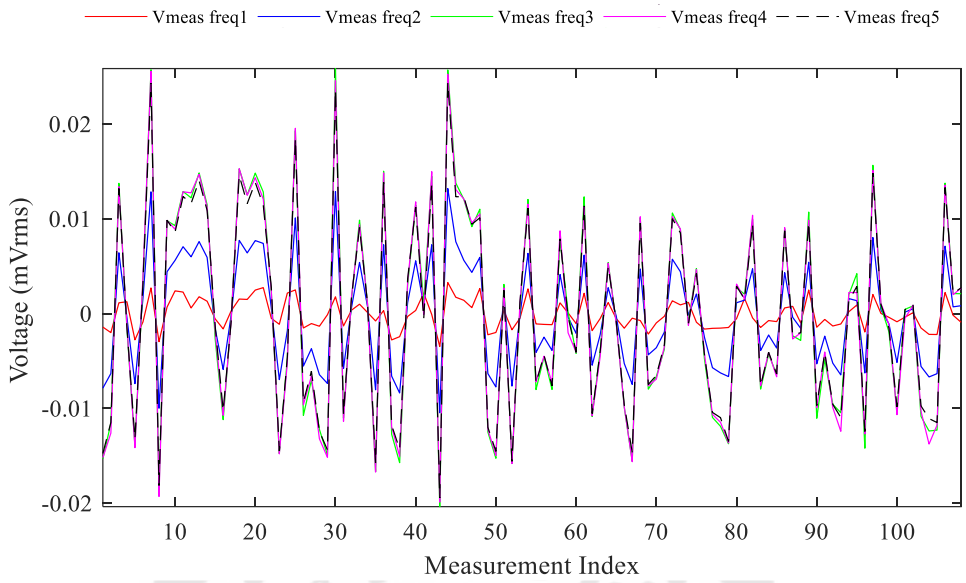

Figure 47 The voltage measurement of 7-electrode probe case.

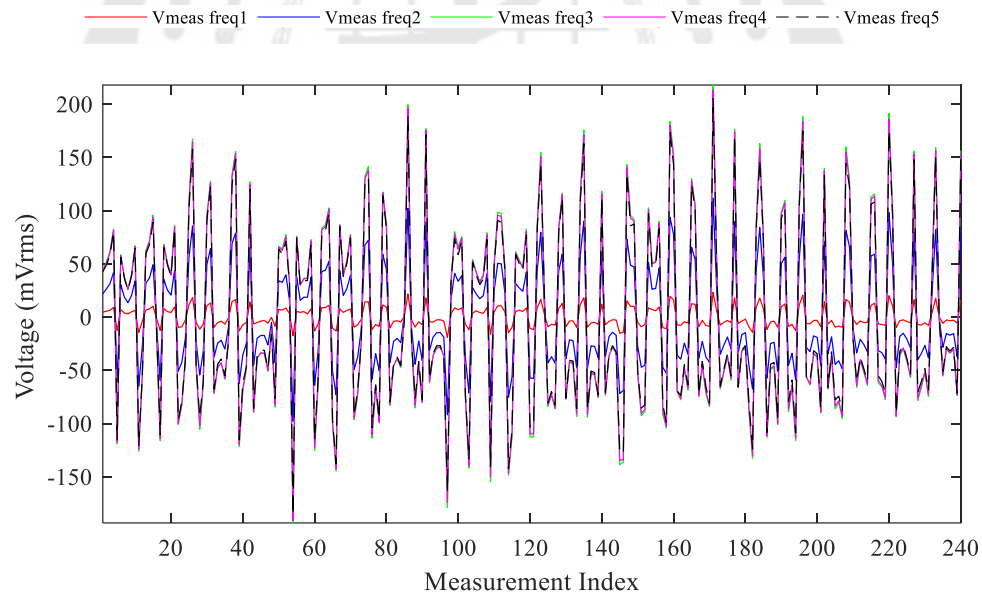

Figure 48The voltage measurement of 16-electrode probe case.

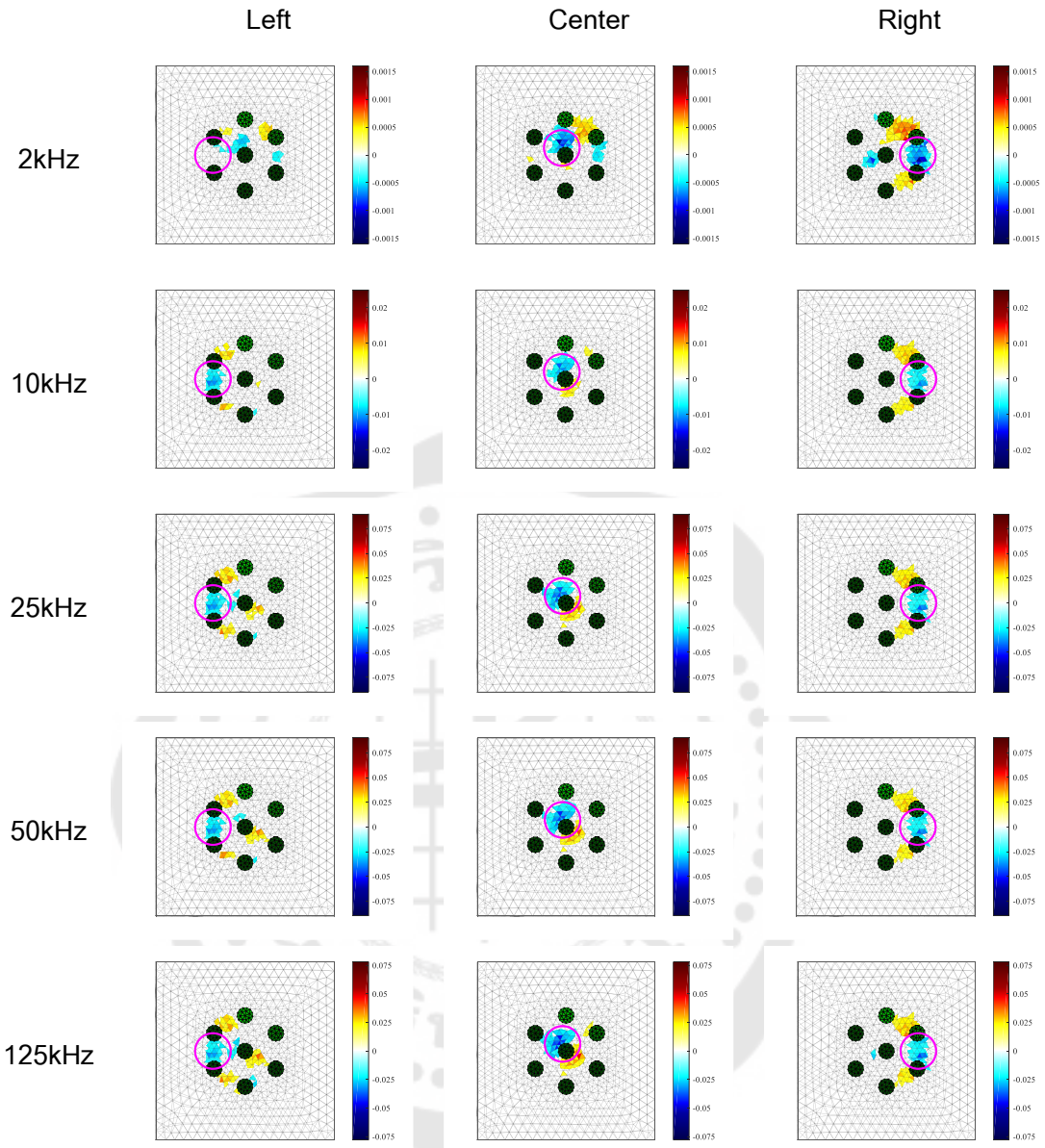

Figure 49 Reconstruction image of the 7-electrode probe case. The magenta circle is the true location of the burn marker.

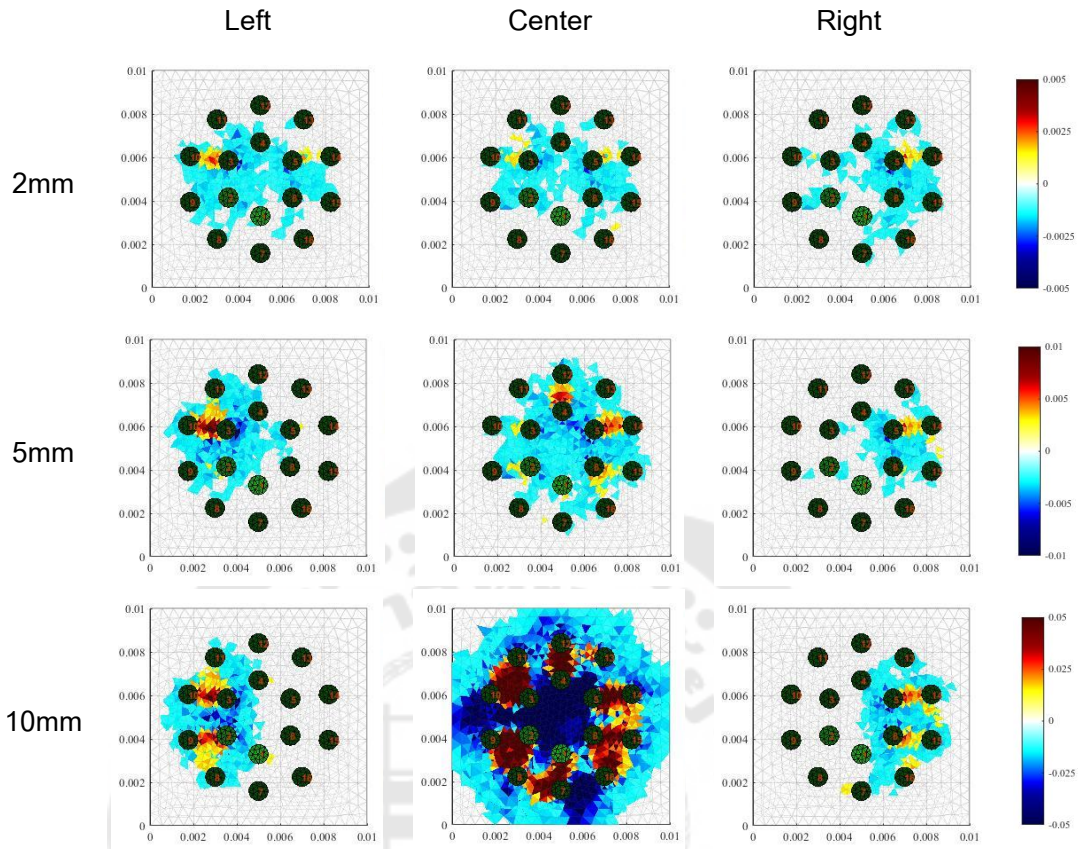

Figure 50 Reconstruction image of the 16-electrode probe case at various cucumber slice size for 2 mm to 10 mm.

Figure 49-50, both probes can locate the conductivity change on the surface. The negative conductivity change was found. Due to the area of electrode array of the 7-electrode probe, it may not be limited to see the change.

4.4 Cervix experiment

From section 4.3, The 16-electrode probe have provided a clearer visualization of the position of the cucumber both for the single-frequency measurement and the multi-frequency measurement. In this section, the multifrequency measurement was selected for the cervix experiment.

Five cervical specimens were used in this study, where case 1 and case 2 were failed due to an inappropriate configuration. For the failed cases (Case 1,2), the setting was based on a current amplitude of ID 1 (0.5 1 2 2 2) and a gain of 2. As a result, the

measurement voltages were over the measurable range of the Clementine EIT machine. In the other cases (Case 3-5), the current amplitude was changed to ID 2 (0.05 0.2 0.4 0.4 0.4) to reduce the reflected voltage amplitude. The experimental results show successful in measurement in regard with the machine capacity.

4.4.1 Configuration of the Clementine EIT machine

Table 5 Configuration of the probe with the Clementine EIT machine.

Case	Setting	Result	note
1	Amplitude ID : 1 Gain : X1.99	At frequency 125 kHz, the voltage measurement was reverse. The amplitude of the current was under the specification due to the over range measurement.	The specimen was quite hard and thick.
2	Amplitude ID : 1 Gain : X1.99	The amplitude of the current was under the specification due to the over range measurement.	
3	Amplitude ID : 2 Gain : X1.99	The voltage measurement at frequency 2 kHz 10kHz 25kHz and 50kHz were a good distribution (determined from the standard division) and the amplitudes of the current were correct.	
4	Amplitude ID : 2 Gain : X1.99		
5	Amplitude ID : 2 Gain : X1.99		

4.4.2 Image reconstruction of cervical specimen

Reconstruction images in three different frequency pairs

In this study, reconstruction was performed using 3 frequency pairs: 50 kHz-2 kHz, 50 kHz-10 kHz, and 50 kHz-25 kHz, where 50 kHz was used as the reference frequency. The experiment is based on the measurement on Case 3 in

quadrant 1. As a result, no significant difference was found on them (Figure 51). For the convenience of result explanation in the next section only the frequency pair of 50 kHz-10 kHz is selected to display (in the part of the comparison with the pathologist's diagnosis).

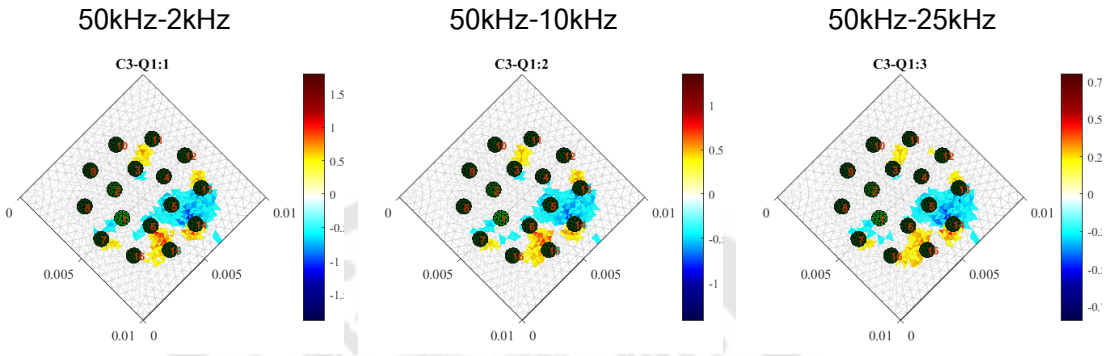

Figure 51 The reconstruction images of the three different frequency pair in case3 quadrant 1.

The reconstruction images of specimens in the comparison with the pathologist's diagnosis

The pathological evaluation of each specimen was performed by dividing the specimen into 4 quadrants (Figure 39). The EIT measurement was perform with the 16-electrode probe when the specimens were uncut (Case 4) or cut in half (Case 3,5). Due to the small space for putting the probe tip, each quadrant was measured or each haft (including 2 quadrants) was measured. Some overlap measurement area was unavoidable. In some cases, the probe was rotated to confirm the image consistency. The reconstruction images were used in comparison with the pathologist's diagnosis (see Figure 52-57). Figures 52, 54, and 56 show the abnormality in the area of the red line, the green as the area where the probe was placed, the orange circle as the area where the specimen was soft which can be determined as the area of the transformation zone, the white circle as the center of the negative conductivity change region (in blue color of the images) in Figures 53, 55, and 57, and the white square as the center of the about-to-unchanged conductivity region in the

reconstruction images (in white color of the images) in Figures 52, 54, and 56. Additionally, the cutting surface was the area with pattern filled as only displayed in Figure 52.

Table 6 Case Diagnosis

	Case3	Case4	Case5
General Information	The second time for LEEP investigation. Investigation for cancer	The first time for LEEP investigation. Investigation for CIN2	The second time for LEEP investigation. Investigation for cancer
Shape	Cup shape	Cone shape	Cup shape
Size	10x15 mm	12x15	15x20
Thickness	4 mm	4 mm	4 mm
Manipulation	Fixed in formalin for 4 hours	Fixed in formalin for 4 hours	Fixed in formalin for 5 hours
Diagnosis	Q1: cancer found at 6 mm length and 2 mm depth Q2: cancer found at 5mm length and 3 mm depth Q3: cancer found at 5 mm length and 4 mm depth Q4: cancer found at 4mm length and 3 mm depth	Q1: CIN 2 found at 4 mm length and 1.7 mm depth Q2: CIN 2 found near Q1 at 5mm length and 0.03 mm depth Q3: not found Q4: not found	This case not found the lesion

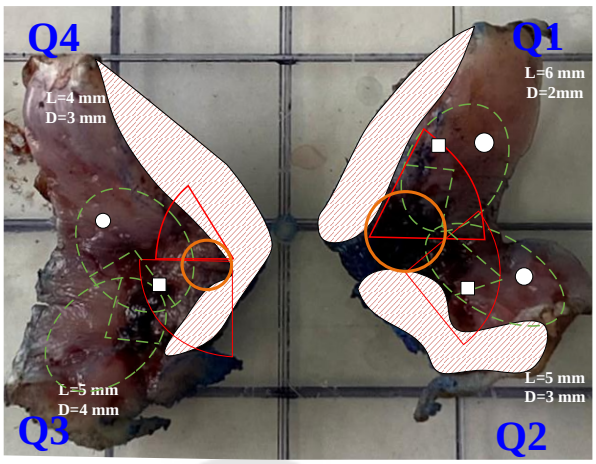

Figure 52 The pathologist diagnosed of Case 3. The area within the red line indicates the area of abnormality, and the green line shows the location of the probe tip. The orange circle is the region of the soft tissue at the orifice.

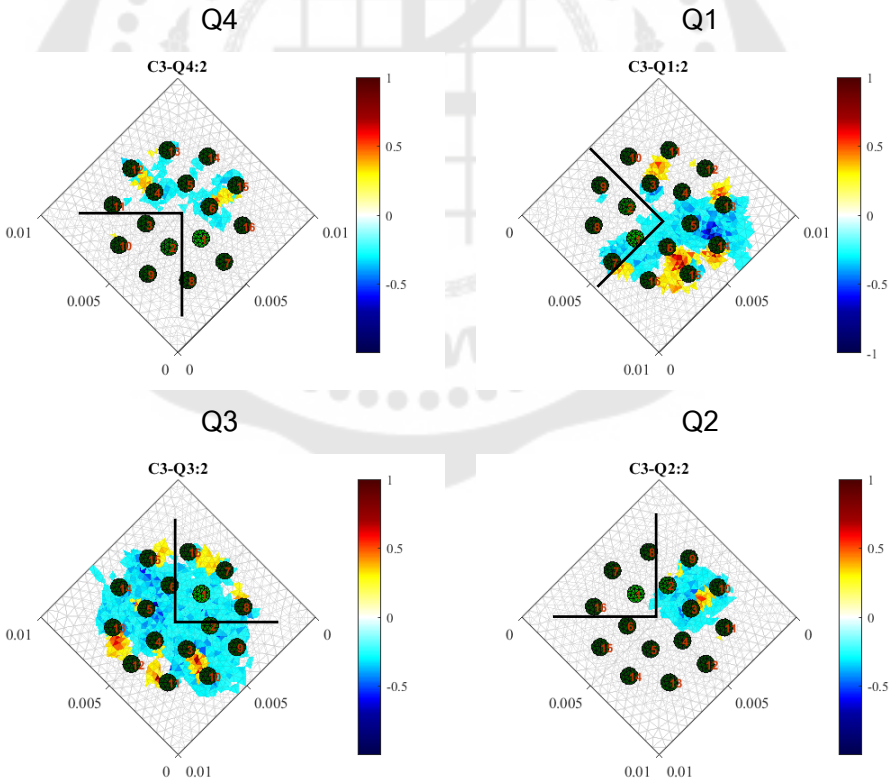

Figure 53 Reconstruction image of the cervical specimen: Case 3.

Case 3 was diagnosed with cancer by the pathologist (see figure 40) in quadrants 1-4, with quadrant 1 (Q1) showing a lesion length of 6 mm and a depth of 2 mm, quadrant 2 (Q2) showing a lesion length of 5 mm and a depth of 3 mm. quadrant 3 (Q3) showing a lesion length of 5 mm and a depth of 4 mm, and quadrant 4 (Q4) showing a lesion length of 4 mm and a depth of 3 mm.

Figure 53 shows the reconstruction image of Case 3. It appears that the white area matched with an area of abnormality, indicating that the blue area was normal region. Since the abnormal cell has an expansion of the nucleus, the current injection at different frequencies did not result in significant difference of conductivity. Apart from the conductivity changing behavior of the abnormal cell, the soft tissue near the cervical orifice has the cell shape that could not cause the large difference of conductivity at different frequencies as well. Therefore, the white region indicates the region of the abnormality or indicates the region of the soft tissue.

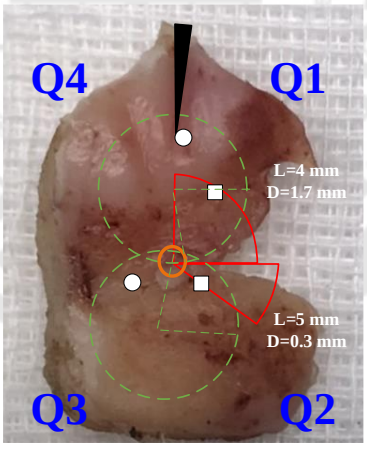

Figure 54 The pathologist diagnosed of Case 4, with the area within the red line indicating the area of abnormality, the green line showing the location of the probe tip, and the black line indicating the incision made by the pathologist. The yellow circle is the region of the soft tissue at the orifice.

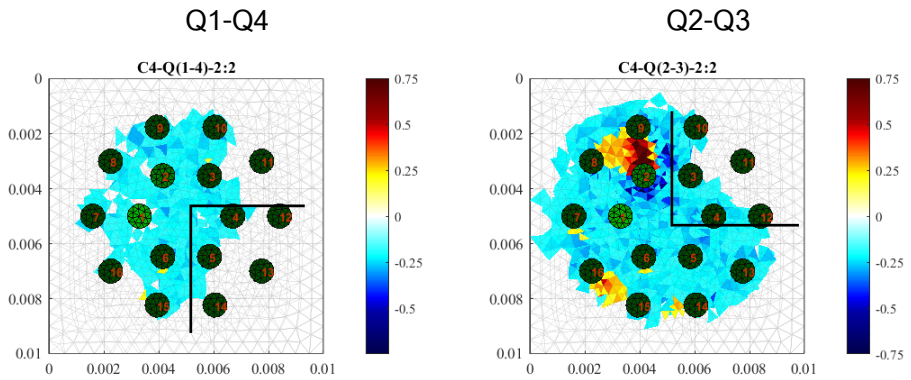

Figure 55 Reconstruction images of the cervical specimen: Case 4.

The pathologist diagnosed case 4 with CIN2 in quadrant 1 and a small area in quadrant 2. Quadrant 1 showed a lesion length of 4 mm and a depth of 1.7 mm, while quadrant 2 showed a lesion length of 5 mm and a depth of 0.3 mm. In this case, the specimen was kept in shape and had a small area of soft tissue near the cervical orifice. Therefore, the white area on the reconstruction images indicates the lesion of CIN2. It is also noticeable that the image amplitudes are smaller than Case 3.

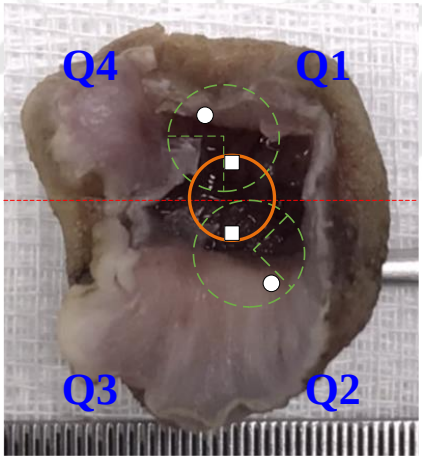

Figure 56 The pathologist diagnosed of Case 5, with the green line showing the location of the probe tip. The orange circle is the region of the soft tissue at the orifice.

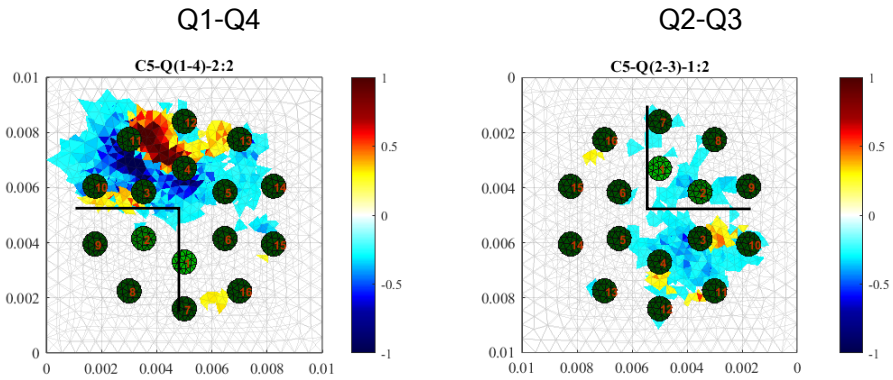

Figure 57 Reconstruction image of the cervical specimen: Case 5.

The pathologist diagnosed case 5 as without a lesion in all quadrants. The reconstruction image of this case shows a clear separation between the blue and white areas. This is because there was a large area of soft tissue around the cervical orifice, which was confirmed to be the reason for the white area on the reconstruction image.

Reconstruction image in single frequency

The reconstruction images based on single frequency was created by the measurement at the back of specimens (the stroma region), as the reference data, and the measurement at the epithelium. The data of the frequency of 25 kHz of Case 4 were selected for demonstrating here. Since the abnormality of Case 4 is CIN2 grade the lesion should reside only in the epithelium region – not in the stroma region, we expected the data obtained from the back of the specimen is the measurement data of the normal tissue. The reconstruction images are showed in Figure. 59. The conductivity changing pattern found in the images is similar to the multifrequency case.

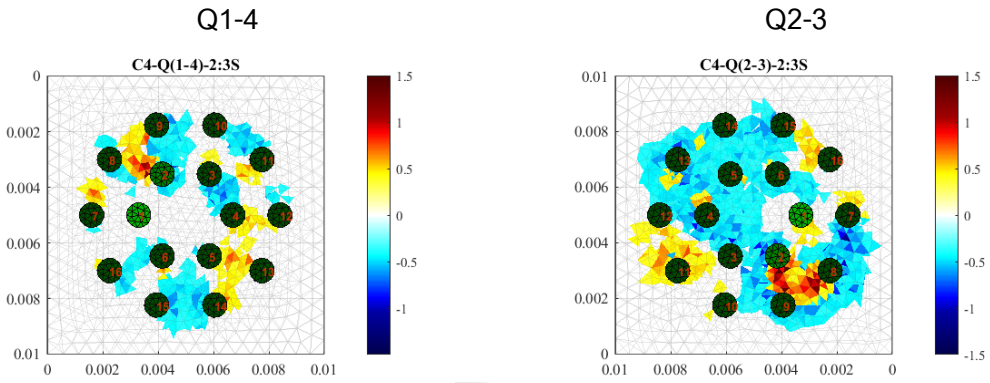

Figure 58 The reconstruction images of 25kHz in case 4.

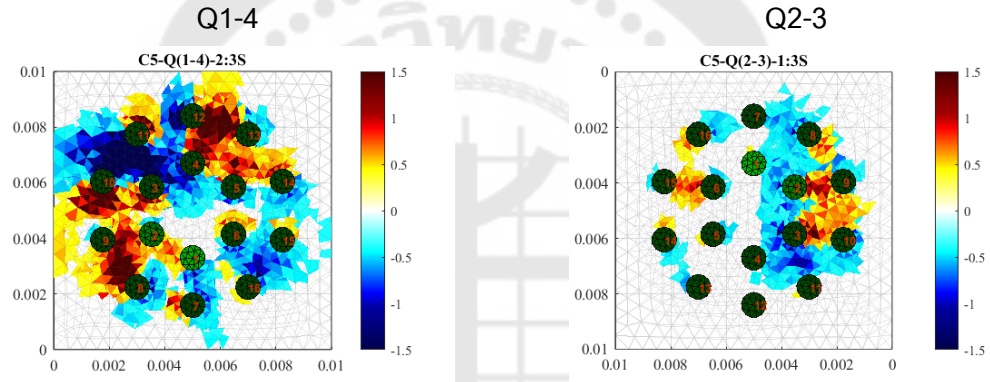

Figure 59 The reconstruction images of 25kHz in case 5.

CHAPTER 5
SUMMARY DISCUSSION AND SUGGESTION

5.1 Discussion

The cervical specimen can be visualized as follows: at the top of the specimen, the soft area is the endocervical region, which is located around the cervical orifice. The next area is the harder tissue, which is the ectocervical region and is the surface of the cervix. The junction between the endocervical region and the ectocervical region is called the transformation zone. Usually, lesions start in this zone and may invade other areas. Finally, at the back of the specimen is the stromal tissue, which is located inside the cervix.

The reconstruction method, in this study we used reconstruction at single frequency and multifrequency. The multifrequency method uses tissue impedance that changes differently over frequency to create an image of conductivity. The image reconstruction shows differences in conductivity that change with respect to frequency. The single frequency method is based on time-difference, uses tissue impedance that varies with time at the same frequency. The image reconstruction shows the change of conductivity in over time. this study, the voltage measurement at the back of the specimen is used as the reference for the time difference.

5.1.1 The configuration of multi-frequency technique

The configuration of the multi-frequency technique on the Clementine EIT machine was used current amplitude ID #2 (0.05 mArms for 2kHz, 0.2 mArms for 10kHz, 0.4 mArms for 25kHz, 0.4 mArms for 50kHz, 0.4 mArms for 125kHz,). Even though the larger amplitude will yield the better sensitivity, it resulted in over range than the machine capacity when measured on the cervical specimens. Empirically, the gain of 2 was suitable for this set of current amplitudes. The phantom studies on a tank, a sausage with a burning marker and with a thin slice of cucumber on the surface were performed to determine the performance of the machine with the regarding configuration. All results show a satisfactory performance.

5.1.2 Conductivity of cervical specimen

The conductivity of cervical specimens was larger than those of in vivo measurement about 2-6 times, investigated on the chamber developed by the author. According to the investigation, the conductivity of the ex vivo specimens was closed to the conductivity of formalin. In fact, the ex vivo specimen was soaked in formalin for 4 hours until it was saturated. The formalin then influenced to the measurement.

5.1.3 Abnormality localization

The localization of abnormality via the multiple frequency technique.

Experimental results show that any pairs of frequencies yielded the similar reconstruction images. However, the pair of 50kHZ (used as the reference frequency) and 10kHz is recommended here due to the high SNR (over 88 dB) and the large number of frequency difference. In this study, the localization performance was determined through visualization, by comparing to the pathologist's diagnosis. The results showed that the unchanged region (the small conductivity change region or the white color region in the image) in the reconstruction image represented the abnormality. Since the abnormal cells deform in shape (to be larger in size) and have large cell space, the conductivity in this region tends to have small change with respect to frequency. This manner is similar to the cell in the transformation zone or the endocervical region. Meanwhile, the conductivity of normal squamous cells tends to have large change respect to frequency, due to the dense layer of cell stack. It causes the negative conductivity change showing in the reconstruction images (negative change region or the blue region).

The localization of abnormality via the single frequency technique.

It is interesting in the case of the single frequency reconstruction that the images are similar to the multiple frequency reconstruction case. Since, the reference measurement was performed at the back (stroma tissue) of the specimen, it could be determined that the stroma cell shape and the cell shape residing in the transformation zone or the endocervical region is similar and has similar electrical characteristic. It is possibly that the conductivity difference between the stroma region and the lesion

region is small as well. Therefore, the images show unchanged in conductivity in the region of the transformation zone or the endocervical region, and possibly the region of lesion. On the other hand, since the cell morphology between the ectocervical region and the stroma region is larger different, the conductivity change then becomes more obvious. This area was then identified as the negative conductivity change in the images (the blue color region).

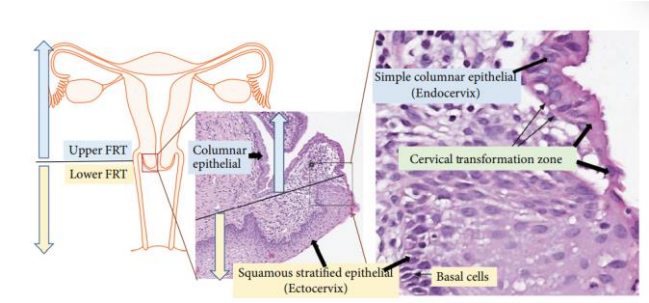

Figure 60 Histology of cervix from Tomasi, J. et al (2019).[32]

Comparison between the 16-electrode probe and the 7-electrode probe

Both probe designs were optimized to provide accurate and reliable measurements, and were tested in various settings. The 7-electrode probe was created earlier, but it was found that the sensitivity region was limited in according the area of the electrode array. The closer distance between the excitation electrode pair also resulted in a high value of voltage measurement that sometime led to over-range measuring. As a result, the 16-electrode probe was later developed to fix the drawbacks of the 7-electrode probe. This probe has a larger tip area and a greater number of voltage measurements, allowing for a more detailed and a precise reconstruction image.

5.2 Conclusion

In this study, two probes were created for detecting cervical precancerous regions in a specimen based on the Multi-frequency EIT technique. The probes were used with a Multi-frequency EIT system, named Clementine EIT. The configuration was investigated in several situations, both on the single frequency and the multiple frequency basis. The investigation included an experiment on a tank by image

reconstructing and comparing voltage measurements obtained from the EIT machine and the estimation using a FEM model, It is also included experiments on biomaterial samples for imaging the inclusion using both probes. A chamber for measuring the conductivity of liquid-based solution was created and the conductivity of formalin was investigated. The conductivity of five cervical specimens fixed in formalin was examined with the 16-electrode probe for using as a parameter for reconstruction. Finally, the 16-electrode probes were used to measure the specimens for locating the abnormality based on the diagnosis provided by a pathologist.

It was found that the 16-electrode probe was suitable for locating the abnormality due to the greater number of voltage measurements (as a result of larger number of electrode) and a larger tip area, which allowed to have more detailed for precise image reconstruction. Regarding conductivity, we found that the conductivity of the ex vivo cervical specimen was higher than that of the in vivo cervical specimen but was close to the conductivity of formalin. This was due to the fact that the ex vivo specimen was soaked in formalin until it was saturated, which influenced the measurement.

The reconstruction was performed with the single frequency and the multiple frequency method. The data of frequency of 2 kHz – 50 kHz were suitable to use for image reconstruction. However, in the case of the multiple frequency method, we recommended to use the frequency of 50kHz as the reference frequency and 10 kHz because of its high SNR (over 88 dB) and the large number of frequency difference. The reconstruction images in the case of the multi-frequency method of the cervical specimens displayed the clearly difference of color region and they are consistent to the pathologist's diagnosis. The unchanged region (white region in the image) represented the abnormality due to the large size of cell and the large cell space. The conductivity in this region tends to have small change with respect to frequency, and the change region (blue region) represented to the normal cells where the cell has large conductivity change with respect to frequency. In the case of the single frequency method, the measurement at the back (stroma region) of the specimens was used as

the reference measurement. The conductivity changing pattern in the images (using a single frequency) was found to be similar to the multifrequency case. This was likely due to the fact that the cells in endocervical region and stromal cells have similar cell shapes, and we can expect the back (stromal region) of the cervical specimen to the normal cell, which can be used as a reference frequency.

In conclusion, the probe can be used for locating the region of abnormality with both the single frequency and the multiple frequency basis. However, the large conductivity change appeared in the images presents the normal region, and the small change presents the abnormality or the endocervical/ transformation region of the cervix.

5.3 Suggestion

Although, the 16-electrode array used was able to locate the abnormality, but it was difficult to place it on the surface of specimens due to its large size. So, using the same number of electrodes but reducing the area of the electrode array (e.g., reduce the array diameter) can improve the usability, and it will be more efficient to place specimens. However, reducing the area of the electrode array may result in a higher voltage measurement value due to the closer distance between the electrodes. The further investigation to make sure the measurement values are in the machine measurement range is necessary.

REFERENCES

1. Sung H, Ferlay J, Siegel RL, Laversanne M, Soerjomataram I, Jemal A, et al. Global cancer statistics 2020: Globocan estimates of incidence and mortality worldwide for 36 cancers in 185 countries. CA Cancer J Clin. 2021;71(3):209-49. 2021/02/05.
2. Duraisamy K, Jaganathan K, Rajendran JCB. Methods of detecting cervical cancer. Advances in Biological Research 5 (4): 226-232, 2011. 2011.
3. Das L, Das S, Chatterjee J. Electrical bioimpedance analysis: A new method in cervical cancer screening. Journal of Medical Engineering. 2015;2015:636075.
4. Abdul S, Brown BH, Milnes P, Tidy JA. A clinical study of the use of impedance spectroscopy in the detection of cervical intraepithelial neoplasia (cin). Gynecol Oncol. 2005;99(3 Suppl 1):S64-6. eng. 2006/02/02.
5. WONGKITTISUKSA B, DOKLONG N. Three dimentional electrical impedance tomography model for breast. 2010(2553).
6. Sillaparaya A, Ouypornkochagorn T. Planar electrode configurations of electrode plates for the localization of cervical abnormality based on electrical impedance tomography (eit) – a simulation study. 2021 11th International Conference on Biomedical Engineering and Technology; Tokyo, Japan. Association for Computing Machinery; 2021. 27–33. https://doi.org/10.1145/3460238.3460243
7. Ousub S, Chumjai P, Sillaparaya A, Ouypornkochagorn T. A simulation study to locate cervical abnormality based on electrical impedance tomography (eit), using a planar nine-electrode probe. 2021 11th International Conference on Biomedical Engineering and Technology; Tokyo, Japan. Association for Computing Machinery; 2021. 1–6. https://doi.org/10.1145/3460238.3460239
8. Jankhaboun S, Janrit W, Ngamdi N, Trongwongsa T, Ouypornkochagorn T. Planar electrode probe patterns for cervical precancerous screening using electrical impedance tomography. 2022 International Electrical Engineering Congress (iEECON). 2022. 1-4.
9. Zhang T, Jeong Y, Park D, Oh T. Performance evaluation of multiple electrodes based

electrical impedance spectroscopic probe for screening of cervical intraepithelial neoplasia. Electronics. 2021;10(16).

10. Hong S, Lee K, Ha U, Kim H, Lee Y, Kim Y, et al. A 4.9 mΩ-sensitivity mobile electrical impedance tomography ic for early breast-cancer detection system. IEEE Journal of Solid-State Circuits. 2015;50(1):245-57.
11. Bera TK. Applications of electrical impedance tomography (eit): A short review. IOP Conference Series: Materials Science and Engineering. 2018;331(1):012004.
12. Vlamos P, editor. Applications for electrical impedance tomography (eit) and electrical properties of the human body. GeNeDis 2016; 2017; Cham: Springer International Publishing.
13. Holder D. Electrical impedance tomography (eit) of brain function. Brain topography. 1992;5:87-93.
14. Manga SM TA, Huh WK, Ngalla C, Liang MI. Type 3 transformation zone of the cervix and risk of missed lesions during cervical cancer screening with visual methods: A case report from cameroon. Obstet Gynecol Cases Rev. 2021;8(2).
15. Russomano F, Tristao MAP, Côrtes R, de Camargo MJ. A comparison between type 3 excision of the transformation zone by straight wire excision of the transformation zone (swetz) and large loop excision of the transformation zone (lletz): A randomized study. BMC Womens Health. 2015;15:12-. eng. 2015/02/18.
16. Cervical cancer. Mayo clinic; 2021 [Available from :https://www.mayoclinic.org/diseases-conditions/cervical-cancer/symptoms-causes/syc-20352501
17. Walker DC, Brown BH, Blackett AD, Tidy J, Smallwood RH. A study of the morphological parameters of cervical squamous epithelium. Physiol Meas. 2003;24(1):121-35. eng. 2003/03/15.
18. Vara JA, Portela A, Ortín J, Jiménez A. Expression in mammalian cells of a gene from streptomyces alboniger conferring puromycin resistance. Nucleic Acids Res. 1986;14(11):4617-24. eng. 1986/06/11.
19. Cervical cancer. Cleveland Clinic; 2022 [Available from :

https://my.clevelandclinic.org/health/diseases/12216-cervical-cancer

20. Cervical biopsy. Sukhi Pariwar Clinic; 2017 [Available from: http://sukhipariwarclinic.com.np/cervical-biopsy/
21. Clinic C. Cone biopsy. 2022 [https://my.clevelandclinic.org/health/diagnostics/23381-cone-biopsy
22. Hysterectomy. NHS; 2022 [Available from : https://www.nhs.uk/conditions/hysterectomy/
23. Kanngoen S. Principle and technique of pathology. 2022 [Available from : https://www.rcst.or.th/web-upload/filecenter/51/19-p.%20411-434.pdf
24. Brown BH, Tidy JA, Boston K, Blackett AD, Smallwood RH, Sharp F. Relation between tissue structure and imposed electrical current flow in cervical neoplasia. Lancet. 2000;355(9207):892-5. eng. 2001/02/07.
25. Malone E, Santos GSd, Holder D, Arridge S. Multifrequency electrical impedance tomography using spectral constraints. IEEE Transactions on Medical Imaging. 2014;33(2):340-50.
26. Goren N, Avery J, Dowrick T, Mackle E, Witkowska-Wrobel A, Werring D, et al. Multi-frequency electrical impedance tomography and neuroimaging data in stroke patients. Scientific Data. 2018;5:180112.
27. Smits FM. Measurement of sheet resistivities with the four-point probe. Bell System Technical Journal. 1958;34:711-8.
28. Schroder D. Semiconductor material and device characterization. Piscataway NJ: IEEE Press; 2006.
29. . Single source current drive patterns for electrical impedance tomography. 2010 IEEE Instrumentation & Measurement Technology Conference Proceedings; 2010.
30. Rajaguru H, Rathinam P, Singaravelu R. Electrical impedance tomography (eit) and its medical applications: A review. Int J Soft Comp Eng. 2013;3:193-8.
31. Liu K, Wu Y, Wang S, Wang H, Chen H, Chen B, et al. Artificial sensitive skin for robotics based on electrical impedance tomography. Intelligent Systems. 2020:1-13.

32. Tomasi J, Opata M, Mowa C. Immunity in the cervix: Interphase between immune and cervical epithelial cells. Journal of Immunology Research. 2019;2019:1-13.

VITA